Abstract

Mallapragada, Vishnu Goutham. Online lignin sensor for high speed sorting of newsprint from recovered paper. (Under the direction of Dr. M. K. Ramasubramanian)

A compact fluorescence based sensor for real time measurement of lignin content in paper has been developed to automate the sorting of newsprint from mixed waste. Lignin content predicted using this sensor correlates well with actual lignin content. However, as a binary sensor to identify low and high lignin content, the sensor works extremely well.

Effects of various parameters such as excitation wavelength, filter bandwidth and color were studied. These results were used to optimize the performance of the sensor. A commercial trial on a moving conveyor was carried out and the results were satisfactory.

Sensor response depends on the distance between the paper sample and the sensor head. In real-time, distance between paper samples and sensor head varies depending on the thickness of paper on the conveyor. Hence, a cascaded solenoid system has been developed to move the sensor head. Calibration curves in combination with sensor head movement make the sensor very effective over a wide range of distances.

Motorola HC12 micro controller interface is provided to the sensor for analog to digital conversion, computation and serial communication to a PC. Sensor output can be monitored at a remote location away from the sorting conveyor.

The sensor is capable of identifying news print samples moving at a speed of 1200 feet per minute.

Online lignin sensor for high speed sorting of newsprint from recovered paper

by

Vishnu Mallapragada

A thesis submitted to the Graduate Faculty of

North Carolina State University

in partial fulfillment of the

requirements for the degree of

Master of Science

Mechanical Engineering

Raleigh, North Carolina

July 2004

APPROVED BY:

Dr. Richard Venditti	Dr. Kara Peters
(Committee member)	(Committee member)

Dr. M. K. Ramasubramanian

(Chair of Graduate Advisory Committee)

Biography

I was born and raised in the South Indian city of Hyderabad. After high school, I started undergrad in mechanical engineering at the Indian Institute of Technology, Madras. In May of 2002, I completed my bachelor's degree with a minor in Computational Solid Mechanics.

Immediately after that, I began graduate school at N C State. I will graduate with my master's in the summer of 2004. My next step is to pursue a PhD at Vanderbilt University, Nashville, TN starting in fall of 2004.

Acknowledgements

I would like to thank Dr. Ram for giving me a fascinating project to work on. His support and advice were invaluable during the course of the project.

Thanks also to Dr. Venditti for letting me use the resources of the Wood and Paper Science department for some of the experiments. His input regarding the effect of color on the sensor was tremendously useful.

I also want to thank Robert Hughes for helping me with the machining of the parts. His comments on the design of the solenoid system were extremely helpful.

This project would not have been possible without funding from the Department of Energy. I would like to thank DOE (award # DE-FC36-00ID13880) for their continued support.

Table of contents

List of Tables

List of figures

List of symbols

h	Planck's constant ($6.63*10^{-34}$ J.s)
c	Speed of light ($3*10^{8}$ m/s)
λ	(Lambda) Wavelength (m)
N	Avogadro's number ($6.24*10^{18}$)
C	Damping constant (N.s/m)
K	Spring constant (N/m)
g	Acceleration due to gravity (9.8 m/s^2)
M1	Mass attached to solenoid A (kg)
M2	Mass attached to solenoid B (kg)
M3	Mass attached to solenoid C (kg)
X1	Displacement of mass M1 (m)
X2	Displacement of mass M2 (m)
X3	Displacement of mass M3 (m)
X4	Plunger length of solenoid A (m)
X5	Plunger length of solenoid B (m)
X6	Plunger length of solenoid C (m)
$X1^{o}$	Velocity of mass M1 (m/s)
$X2^{o}$	Velocity of mass M2 (m/s)
$X3^{o}$	Velocity of mass M3 (m/s)
$X1^{oo}$	Acceleration of mass M1 (m/s^2)
$X2^{oo}$	Acceleration of mass M2 (m/s^2)
$X3^{oo}$	Acceleration of mass M3 (m/s^2)
F1	Force exerted by solenoid A (N)
F2	Force exerted by solenoid B (N)
F3	Force exerted by solenoid C (N)
L	Distance moved by solenoid A (m)
E	Energy (Joules)

Acronyms

NPS	Newsprint
WLP	White ledger paper
KP	Kraft paper
TMP	Thermo mechanical pulp hand sheet
CP	Copy paper
MP	Market pulp
QE	Quantum efficiency
NM	Nondimensionalized mass

1. Introduction

Before waste paper is recycled at a paper mill, it is sometimes sorted at a recycling center (or at paper mills with a sorting facility). Waste paper is sorted broadly into the following categories.

1. Glossy paper
2. Office paper
3. Colored paper
4. Cardboard
5. Newsprint
6. Mixed waste

Glossy paper typically consists of magazine or coated paper. They have a heavy coating that some paper mills do not accept. It has to be treated separately before recycling.

Office paper is usually made from high-grade paper pulp and consists of letterhead, ledger, notebook, computer paper etc. It requires less processing than other grades of paper.

Colored paper has to be bleached to remove the dyes before recycling. Hence it has to be separated from non-colored paper during the sorting process.

Cardboard generally refers to corrugated cardboard and boxboard. Corrugated cardboard is made of three layers and is used for packing and shipping containers. Boxboard is used to make cereal boxes, folding cartons etc. These are made of low-grade paper and are mostly recycled to make more cardboard.

NPS is made of low-grade paper and cannot be mixed with office paper, as it would decrease the quality of recycled paper. Hence it has to be sorted separately.

Mixed waste consists of paper that cannot be separated into any of the above categories. It usually goes to a landfill.

Currently sorting of waste papers, according to grades prior to recycling, is done manually in municipal waste sorting plants, where the paper waste is broadly classified as brown cardboard, newspaper and mixed office waste. Manual sorting is very inefficient in terms of both accuracy and throughput. Hence there is a need for an automated waste paper sorting system [1]. Figure 1.1 shows a schematic of an automated system.

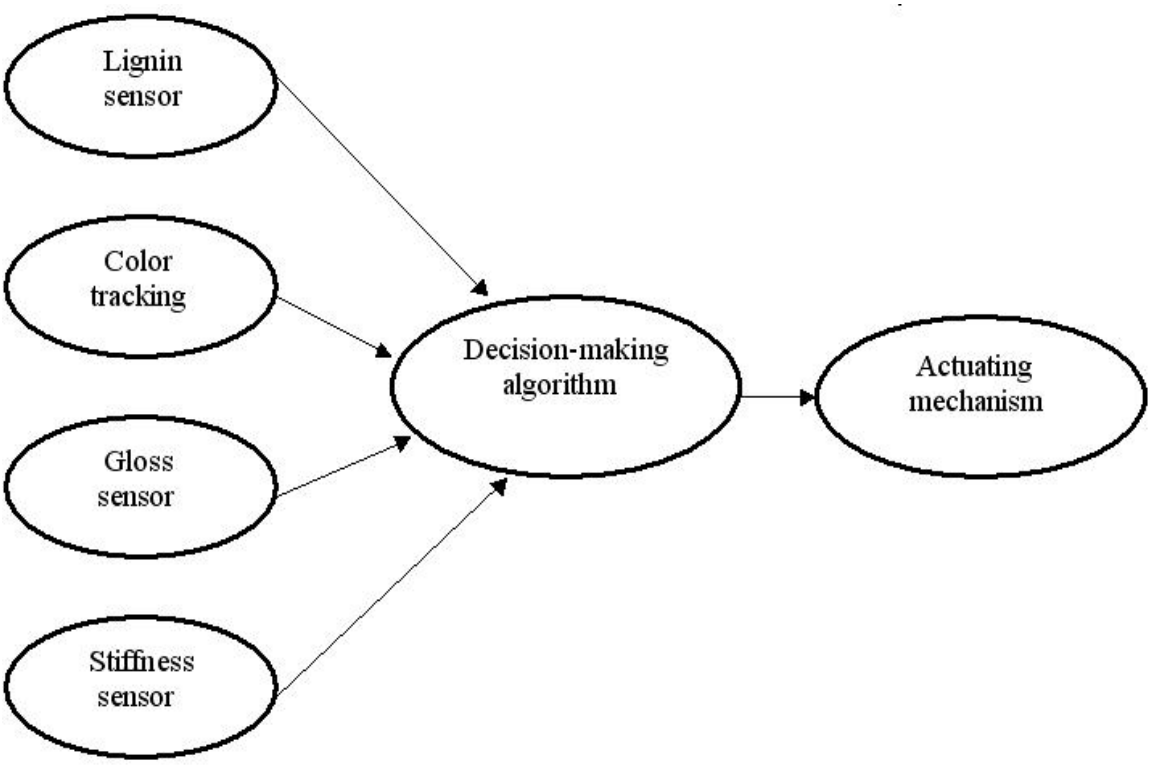

Figure 1.1. Automated sorting system

The concept of a stiffness sensor is to measure the relative stiffness of various paper samples using optical techniques. This is used to sort cardboard from other types of paper. Lignin sensor measures the lignin content in the paper sample. This is used to sort newsprint from mixed office waste. Color tracking system gives information about the color of the paper sample. Gloss sensor measures the glossiness of the paper surface.

Data from these sensors is used by a decision-making algorithm to categorize the paper sample and actuate a sorting mechanism.

If a sample gives high sensor output from one sensor and low sensor output from other sensors, then the categorization is straightforward. A decision making process is essential when a sample gives significant output from more than one sensor. For instance, consider a newsprint sample with areas of printed color on the surface. Depending on the amount of color and lignin content, a decision has to be made on the categorization of the sample.

This thesis describes the design and implementation of the lignin sensor as part of a multi sensor system for paper sorting.

2. Background

Wood is made of three major components, cellulose, hemi cellulose and lignin. Wood is pulped by either a mechanical process in which the wood chips are literally ground to individual fibers or chemically pulped to dissolve the lignin holding the fibers together to release individual fibers. Typically, lignin comprises 20-30% of wood [5]. Lignin is a three dimensional branched polymer polymeric material with phenyl propane as the basic unit linked by different kinds of bonds with each other, as illustrated in Figure 1 [6].

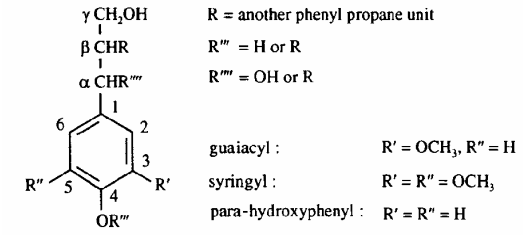

Figure 2.1. Basic Structural unit of Lignin polymer [6]

The mechanical pulping process can be carried out under heated conditions, called the thermo-mechanical process. The pulp is dull gray but a bit yellow due to photo degradation of lignin over time. This type of inexpensive pulp is mostly used in newspapers and catalogs and contains high amounts of lignin. The chemical pulping process is known as the kraft process. In the Kraft cooking process most of the lignin is removed from the wood by chemically active cooking liquors. The resulting fibers, termed unbleached kraft pulp, are strong and brown, most often used in corrugated containers. The brown color is produced by degraded lignin remaining in the fibers. The kraft pulp can be bleached to produce high brightness pulp called bleached kraft pulp, which is white and bright [7]. The fibers are often used in printing papers, such as copy paper and writing paper. Fully bleached wood pulp will have lignin content as low as 0.1% [5].

In recycling it is important to keep these three types of fibers separate and to recycle them separately. Papers made with mechanical pulps are typically recycled back into

newspaper material and therefore require the removal of ink and other contaminants during recycling. These types of paper are often bleached to improve their brightness. Similar types of de-inking and bleaching steps are used to convert paper based on bleached kraft pulps into printing and writing grades. In contrast, paper made with unbleached kraft is not typically de-inked or bleached, as it is used to make recycled brown boxes and containers. Brown unbleached kraft fibers are not appropriate for printing and writing purposes as they decrease the brightness of the paper. Mechanical pulps cannot be tolerated in the production of bright writing papers such as copy paper as the copy paper would unacceptably yellow over time. There are even manufacturing issues and problems with product uniformity and product strength if bleached kraft pulp is incorporated into newspaper or corrugated containers in an uncontrolled manner. Thus, a key challenge is to produce relatively homogenous streams of these three types of fibers from wastepaper sources to improve the recycling efficiency. Hence, sorting of waste paper based on lignin content prior to fiber recovery is essential for efficient recycling.

A review of the fluorescence spectroscopy of lignin and cellulose, two of the major components of paper fibers, is given in reference [8]. Toner and Plitt [9] reported a comprehensive study of the fluorescence of cellulose from cotton. Fluorescence emission was observed visually and the study concluded that the fluorescence emission spectrum was broad, and contained a single maximum at 365 ± 5 nm for excitation wavelengths ranging from 240 to 355 nm. It is well established through steady-state and single-photon timing fluorescence experiments performed on thin sections of Abies wood that the luminescence of emission of wood is from the fluorescence of lignin present [10]. Several investigators have used fluorescence to measure lignin content in pulp and pulping liquor [11-19]. Generally, excitation wavelength in the ultraviolet region and fluorescence measurement in the visible region have been used. Hanson and Wenzel [15] measured laser-induced fluorescence of lignin with excitation from 457 to 621 nm wavelengths when kraft lignins were redissolved in alkali. They report that more sensitive photon count settings are required at higher excitation wavelengths. For excitation at 582 nm, their results show peak fluorescence intensity at 660 nm. Bergstrom et al. [3] used time

resolved and fluorescence microscopic techniques to identify several components of newsprint and recycled furnishes. Under ultraviolet illumination fluorescence emission was observed from the fine paper filler and fluorescence-whitening agent. The emission from the filler (calcium carbonate) was attributed to small amounts of fluorescence impurities and not to the calcium carbonate. Lignin was the only isolated constituent to emit fluorescence under visible illumination.

Figure 2.2 shows the fluorescence spectrum with an excitation wavelength of 532 nm [1]. It can be observed from the graph that significant fluorescence is in the 620 nm – 680 nm bandwidth.

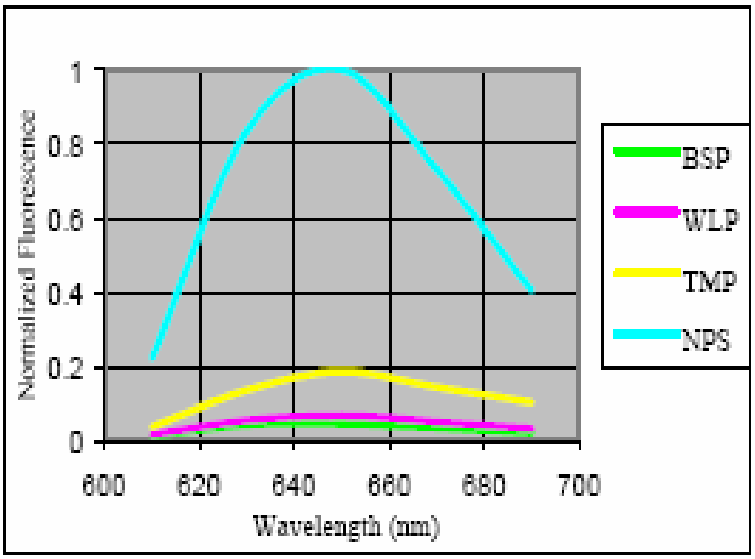

Figure 2.2. Fluorescence spectrum

Fluorescence in newsprint has been studied by Bergstrom, Carlsson, Hellentin, and Malmquvist [4, 19] at excitation wavelengths 337 nm, 570 nm, and 670 nm. They concluded that at higher wavelengths, the effects of fluorescent whitening agents are insignificant and the fluorescence observed is from lignin. They subsequently reported a red fluorescence sensor with an excitation wavelength of 630 nm and they recorded the fluorescence from 660 to 740 nm [4, 19]. They report a Gaussian distribution of fluorescence intensity versus distance of the sample from the sensor, with a maximum intensity occurring at 15 mm. 1% variation in distance can lead to 10% variation in

fluorescence intensity measured. They report a special resolution of 20µm on a full-scale production line. The sensor is mounted to maintain constant distance from the sample by mounting in regions where the paper goes over a roll. However, they did not report direct correlations between measured intensity and actual lignin content in the sheet. In pulping liquors, Bublitz et al. [13, 14] demonstrated that fluorescence intensity was proportional to the quantity of lignin present and the intensity was linearly related to the lignin concentration up to 15 parts per million.

To develop an efficient sorting system, robust sensors that can distinguish between various types of paper based on optical and physical properties are required. A lignin sensor that can differentiate newsprint from other paper types has been presented in [1].

2.1. Lignin sensor design

When excited with a light source lignin gives off fluorescence at a higher wavelength than that of the source. The intensity of fluorescence depends on the amount of lignin present in paper. A lignin sensor measures the intensity of fluorescence to predict the amount of lignin present in paper. Figure 2.3 [1] gives the schematic of the lignin sensor.

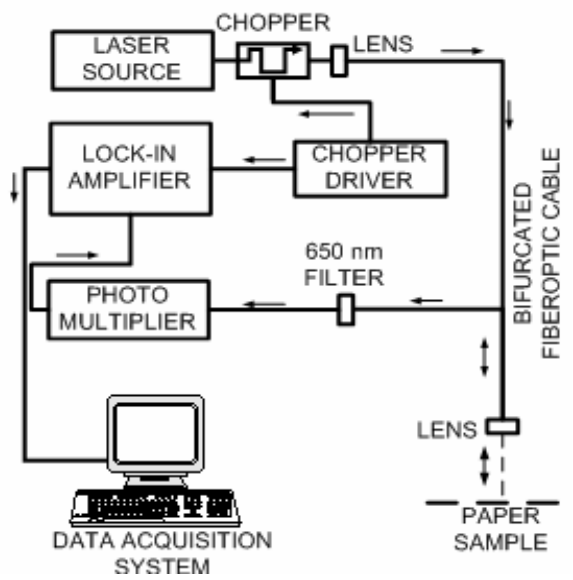

Figure 2.3. Lignin sensor [1]

The visible light source is a pumped diode solid state laser (Power Technology Inc, Model: LCS-DTL-312), 532nm, 50mW peak power with CW mode of operation and intracavity frequency doubling. Laser light is focused on the paper sample using a biconvex lens. The light is chopped using an optical chopper (SR540, Stanford Research Systems) before entering a bifurcated optic fiber cable (Ocean Optics, R200-7-UV/VIS), which has six fibers 200μm diameter arranged around a fiber in the center. The center fiber is used for the excitation source and the six surrounding fiber bundle is used for collecting the emission fluorescence. The fluorescence emitted is collected through a 650 nm filter and presented to a photo multiplier (Multialkali Perkin Elmer CPM 962 with a spectral response from 165nm-850nm) for intensity measurement. A high voltage power supply (Perkin Elmer CHV 30N) was used to power the photo multiplier. The chopper and the photo multiplier signal were synchronized with a lock-in amplifier (Stanford Research Systems, SR530). The output of the lock-in amplifier is interfaced to a data acquisition personal computer using Lab View software or simply measured using a digital storage oscilloscope. For the excitation wavelength of 532nm, chopper frequency of 1500 Hz, laser output power of 50mW, sample to fiber optic sensor tip of 70mm, fluorescence intensities were measured for different samples.

A series of experiments were conducted to characterize the behavior and performance of the lignin sensor for high speed sorting application. The effects of ink/toner on the surface of the paper, color of the base-paper, the basis weight of the sample, the effect of laser excitation power, and the effect of sample distance were presented in [1]. Further, the dynamic performance of the sensor when samples were in motion at 3.7 m/min. was reported.

2.2. Objectives

The experimental sensor design presented earlier is very effective, but not suitable for industrial applications. Hence, this work was undertaken to meet the following goals:

- Design a compact, robust and easily transportable sensor
- Integrate a versatile data acquisition system into the sensor
- Configure the sensor for serial communication with a PC at a remote location
- Calibrate the sensor to correct for varying heights of paper samples
- Design and build an actuating system for sensor head movement
- Test the usefulness of the sensor in measuring absolute lignin content
- Understand the effect of printed text and color on lignin response

3. Absolute lignin measurement

Sensor output from the experimental setup is a voltage signal between 0 – 10 volts. Before operation, sensor is calibrated by adjusting the gain of the photo multiplier tube. Gain is set so that a standard laboratory hand sheet (5.2 grams, 100% NPS) gives a maximum output of 10 volts. Taking ratios of all measurements to 100% newsprint sample measurement, and thus normalizing the data accounted for the overall stability of the photo multiplier. When the photo multiplier output degrades over time from continuous use, the ratio will remain constant. This ratio gives the normalized lignin content in paper. To measure the absolute lignin content, experiments were carried out with the laboratory sensor first to establish the relationship between klason lignin (acid insoluble lignin) content in pulp and the sensor output. This section describes the experiments with the laboratory sensor and the results.

3.1. Preparation of hand sheet samples

Samples of various proportions of standard unprinted virgin newspaper and fully bleached chemically pulped hardwood market pulp mixtures were made into hand sheets. Both the newsprint and the market pulp were soaked in water for 10 minutes, blended and disintegrated using a Tappi Disintegrator for eight minutes at 5% consistency. Hand sheets (2 grams +/-5%) were made in a standard Tappi British hand sheet mold but were not pressed. The hand sheets were dried in a speed dryer for four minutes. Hand sheets of the following compositions were made: 100% MP, 75% MP-25% NPS, 50% MP-50% NPS, 25% MP-75% NPS, and 100% NPS.

3.2. Results

The acid insoluble lignin in the mixtures (5% consistency) was measured according to Tappi Standard Method, T 222 om-88. Samples of different weights were also made using the same hand sheet making procedure. Standard TAPPI hand sheets weighing between 43.35 g/sq m and 265.2 g/sq m (0.85g and 5.2g) were made and used in the

experimentation. A hand sheet weighing 0.85 g has lignin content of 10.89 g/sq m and a hand sheet weighing 5.2 g has lignin content of 66.64 g/sq m. A number of trials of fluorescence measurements were made on the prepared hand sheets. Each trial was started afresh by calibrating with the 100% newsprint sample and adjusting the measurement to read close to 10 volts. Samples were tested in random order to ensure no systematic variation in measurements. The results obtained are shown in the Table 3.2.1.

Table 3.2.1. Klason Lignin Content

%Market pulp	% Klason lignin	% Klason lignin
	Tappi Method Actual	Predicted by Sensor
0	25.77	25.77
25	19.8	19.33
50	13.15	12.87
75	6.85	6.43
100	0	0

Figure 3.2.1 shows a plot of the normalized sensor output in the sheet versus percent market pulp. It is seen that the fluorescence intensity decreases as the lignin content in the bulk of the sheet decreases with increasing market pulp in the blend. The repeatability of the data is excellent. The curve fit shown is of third order.

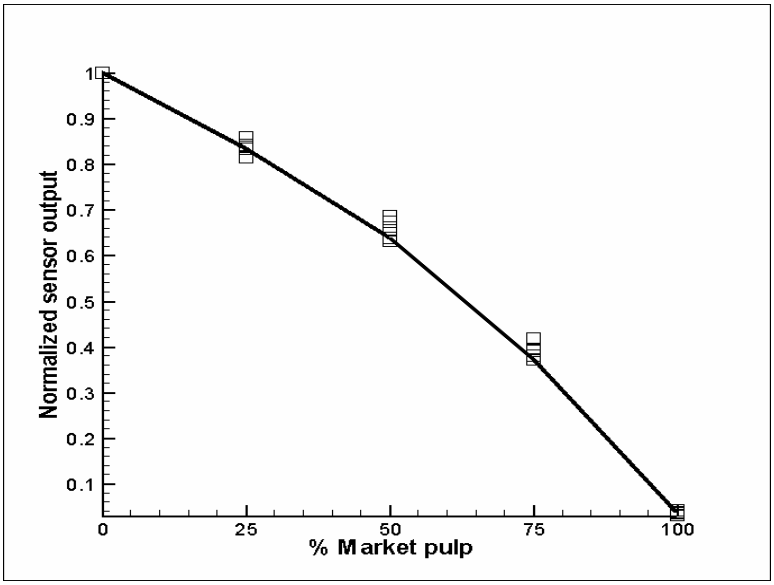

Figure 3.2.1. Normalized sensor output vs. Percent MP

The klason lignin content in market pulp blends versus the normalized sensor output is shown in Figure 3.2.2. The reproducibility of data (indicated by data points at the same lignin content) and the correlation between the lignin content and sensor output are excellent.

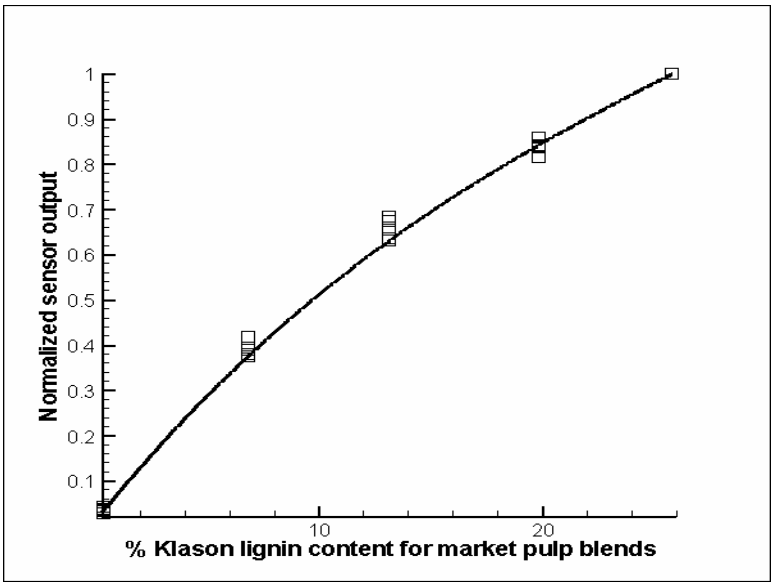

Figure 3.2.2. Klason lignin content in MP blends

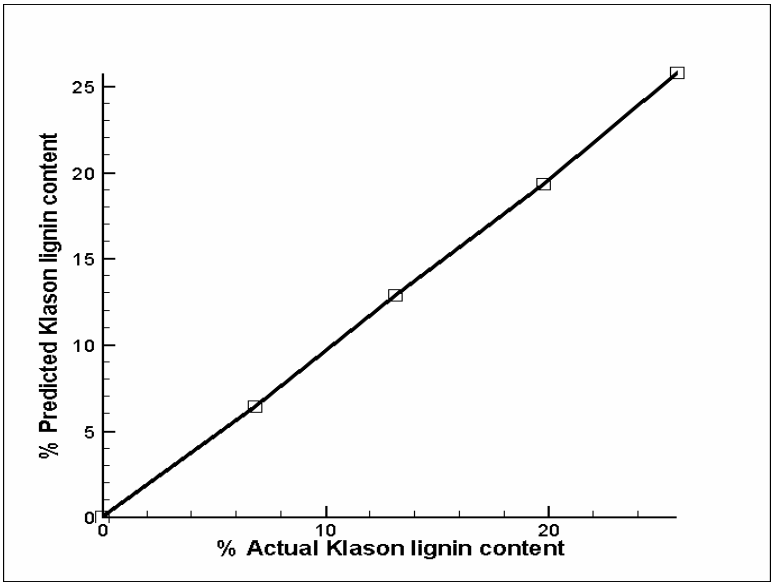

Figure 3.2.3. Klason lignin content comparison

A plot of the lignin content predicted by the sensor output and the Klason lignin content is shown in Figure 3.2.3. The correlation is excellent. Since the percent market pulp and

klason lignin content are related inversely, and the sensor output and lignin content are related directly, it is not surprising that the Predicted and Actual lignin contents show excellent correlation.

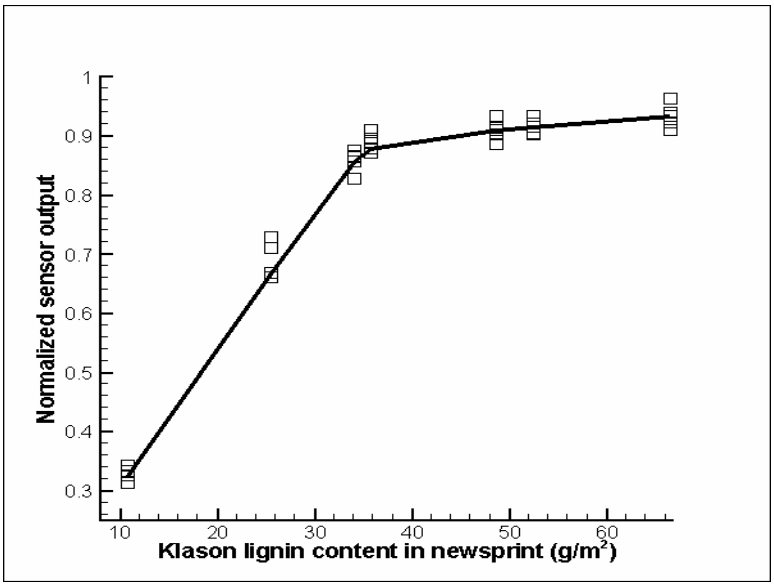

Figure 3.2.4. Klason lignin content in NPS

Figure 3.2.4 shows the effect klason lignin content in NPS without printing on the surface. It is clear that the sensor saturation occurs at about 38 g/m^2. Saturation occurs since the paper sample gives enough fluorescence to get the maximum sensor output even at a lignin content of 38 g/m2. These results were obtained using the green laser source (532 nm) in the laboratory. If the sensor is used for binary sorting, because of saturation the output shows a clear distinction between newsprint and non newsprint paper. Hence, saturated sensor response is better for sorting purposes.

4. Effect of printed text

Paper samples with different quantities of printed text were used to evaluate the effect of print on the sensor output. The samples had 100%, 50% and 0% text printed on them. Only black print was considered. Paper samples of similar thickness and weight were considered (about 0.98g/cm^2 +/- 5%). Copy paper and TMP sheets were used for the experiments. Copy paper was printed with W's tightly packed without any spaces between them, and we call it the 100% printed text surface. 50% printed text on copy paper was achieved by printing W's and spaces alternatively. 0% printed text copy paper was just a blank copy paper. 100% printed text on TMP was achieved by carefully handpicking printed newsprint with maximum density of printed material (mostly W's). 50% printed text on TMP was achieved by picking newsprint with printed text and spaces alternatively. 0% printed TMP was just a section of unprinted newsprint paper. Figures 4.1 and 4.2 show the sample formats used for 100% and 50% printed text.

Figure 4.1. 100% Printed text

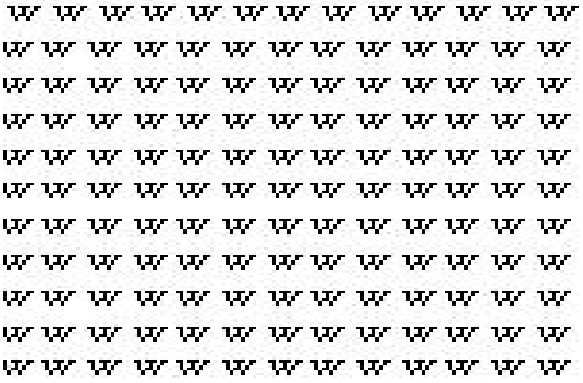

Figure 4.2. 50% Printed text

The samples were tested with the lignin sensor and results are plotted as a bar graph in Figure 4.1. Results show that the print does decrease the sensor output. However, even a fully printed text has coverage of only about 15 %, significant reduction is sensor output was not observed. Hence, the printed text in itself does not pose a problem when identifying newsprint and non-newsprint furnishes.

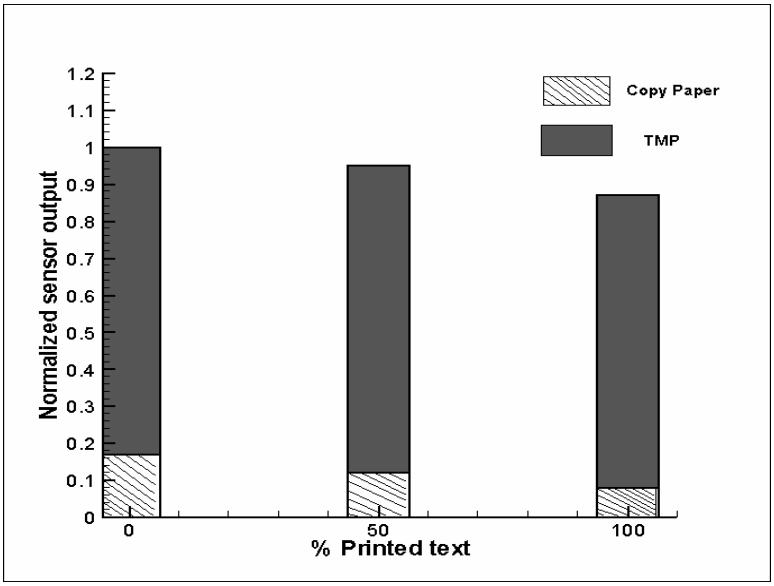

Figure 4.3. Effect of printed text

5. Commercial trial

In order to study the usefulness of the sensor, a commercial sorting trial was run at MSS Inc, Nashville, TN. Lignin sensor was setup over a high-speed industrial conveyor. The sensor was calibrated with a 5.2 gram (basis weight of 265 g/m^2) 100% news print sample. The sensor tip was placed at a distance of 70 mm from the conveyor. Static data was taken when the conveyor was at rest and the dynamic data was taken when the conveyor was moving at 600 feet per minute. Figures 5.1 and 5.2 show the sensor setup.

Figure 5.1. Sensor setup at commercial trial

Figure 5.2. Sensor head over conveyor

Table 5.1 shows the samples that were passed under the sensor and the sensor output. As expected, only the newsprint showed significant sensor output compared to all other grades shown in the list.

Table 5.1. Samples used in commercial trial and sensor output.

Sample Type	Normalized static	Normalized dynamic
	Sensor output	Sensor output
Colored CP	0	0
Cardboard with brown paper on top	0.04	0
Cardboard without brown paper on top	0.04	0
Packing cardboard with glossy coat	0	0
Packing cardboard without glossy coat	0.07	0
Cardboard with white paper on top	0.04	0
Cardboard without white paper on top	0.04	0
Packing cardboard with glossy coat	0.04	0
Glossy magazine paper	0.11	0
Thick glossy magazine paper	0.04	0
Packing cardboard with glossy coat	0.04	0
Packing cardboard without glossy coat	0.07	0
Packing cardboard with glossy coat	0.04	0
Packing cardboard without glossy coat	0.07	0
Thick glossy magazine paper	0.07	0
Glossy magazine paper	0.14	0
Packing cardboard with glossy coat	0.04	0
Packing cardboard without glossy coat	0.09	0
Brown paper	0.04	0
News paper	0.45	0.5
Packing cardboard with glossy coat	0.04	0
Packing cardboard without glossy coat	0.04	0
White CP grid pattern	0	0
Cardboard	0.04	0

6. Compact lignin sensor design

Figure 6.1 [1] shows the sensor setup (from here on this sensor setup will be referred to as the old sensor) used for the experiments.

Figure 6.1. Sensor setup [1]

Though this setup works well and gave excellent results, the design needs to be modified to make it robust and industry worthy. The sensor needs to be compact, rugged, and have only the essential components for lignin identification. Although, the laboratory system works well, it is made up of laboratory general-purpose amplifiers, and light source. It has many components, is extremely bulky and very costly. The wiring and data acquisition with an oscilloscope are suitable for research, but not necessary for industrial application. After a systematic evaluation of all the parts some of them have been eliminated or replaced with more economic and easily transportable components.

6.1. Lock in amplifier

The lock in technique is used to detect and measure very small ac signals. A lock in amplifier can make accurate measurements of small signals even when the signals are obscured by noise sources, which may be a thousand times larger. Essentially, a lock in is

a filter with an arbitrarily narrow bandwidth, which is turned on to the frequency of the signal. Such a filter will reject most unwanted noise to allow the signal to be measured.

The lock in amplifier works extremely well, but it weighs 16 lbs with outside dimensions of 17" X 17" X 5.25". It is extremely bulky and is not suitable for a compact sensor design. Hence a circuit has been designed using a modulator/demodulator chip (AD630 from Analog devices) to replace the lock in amplifier. Figure 6.1.1 shows a schematic of the main circuitry. Figure 6.1.2 shows the circuit diagram.

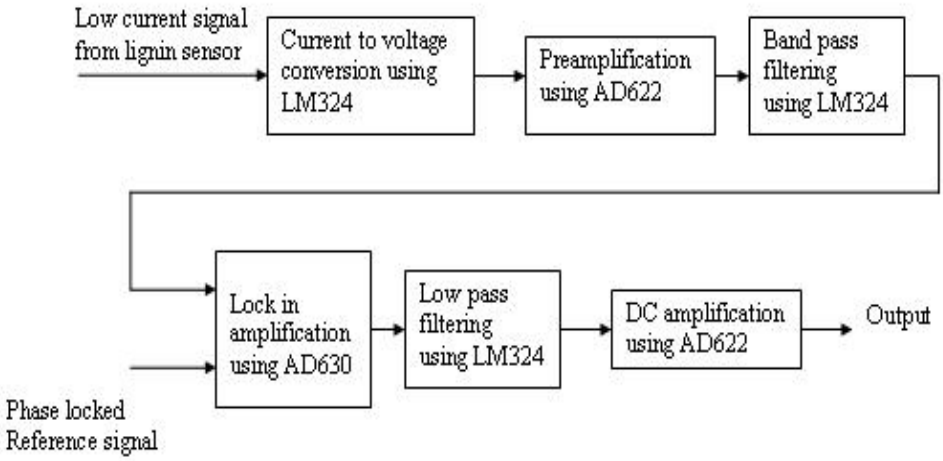

Figure 6.1.1. Lock in circuitry

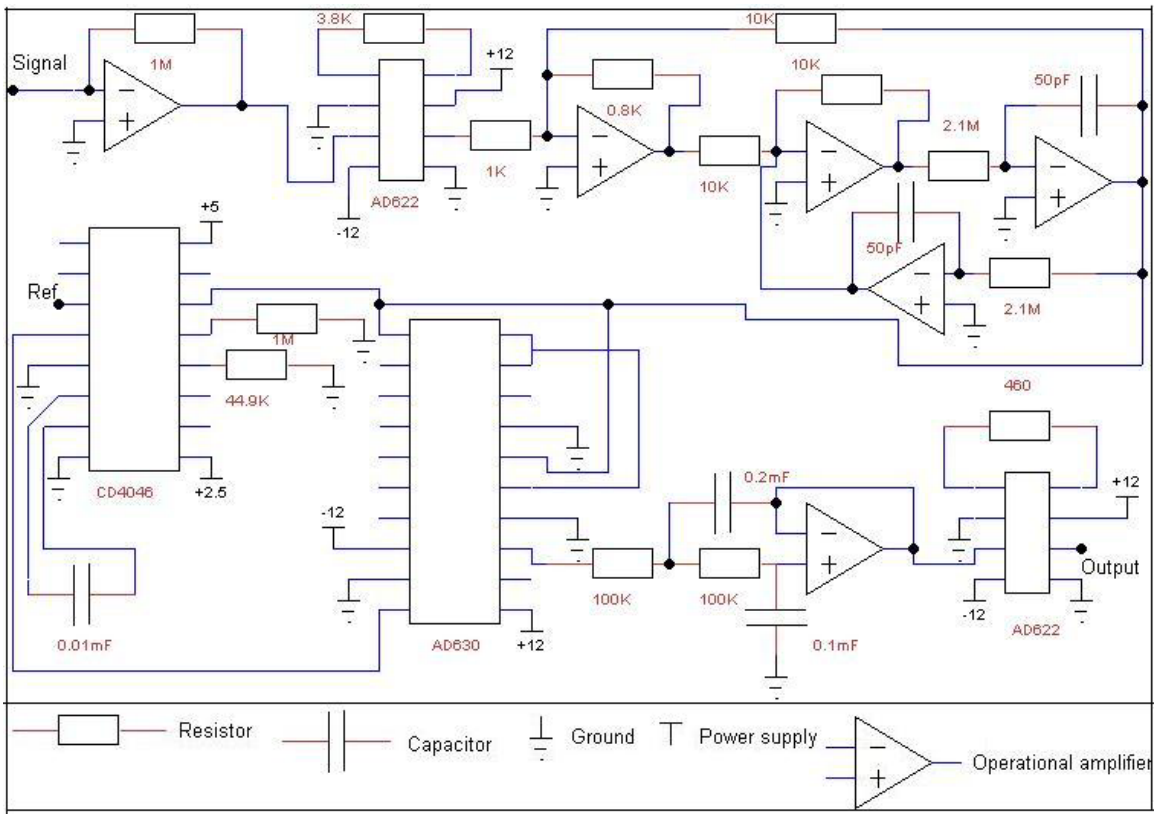

Figure 6.1.2. Lock in circuit layout

Figure 6.1.3 shows the performance of the lock in circuitry compared to the lock in amplifier using newsprint samples. The lock in amplifier performs better than the circuitry as it shows a better gradient in sensor output for varying lignin contents. It is obvious from the figure that both of them saturate at a lignin content of 40 g/sq m.

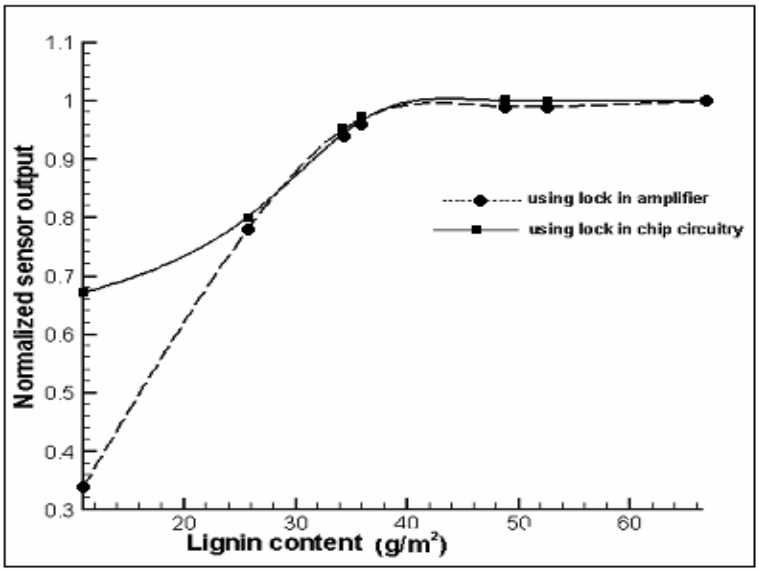

Figure 6.1.3. Comparison for NPS samples

Figures 6.1.4 and 6.1.5 compare the lock in circuitry and amplifier results for CP – NPS and MP - NPS blends.

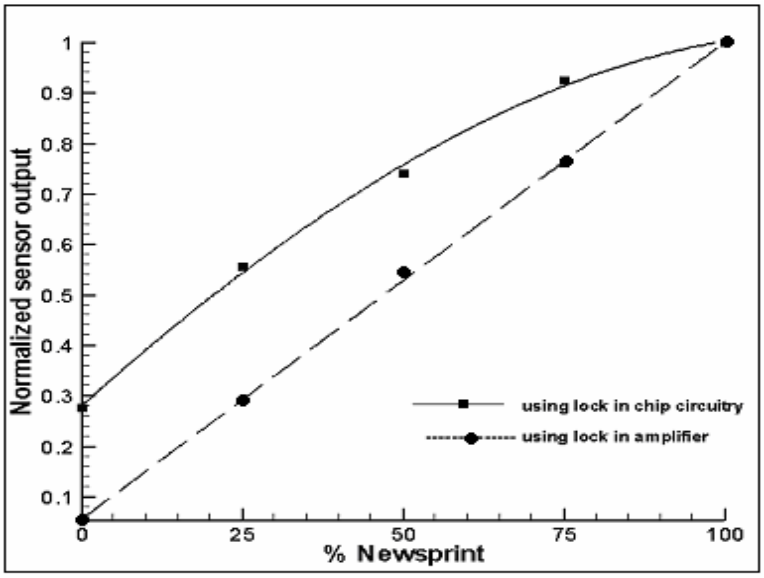

Figure 6.1.4. Comparison for CP - NPS blends

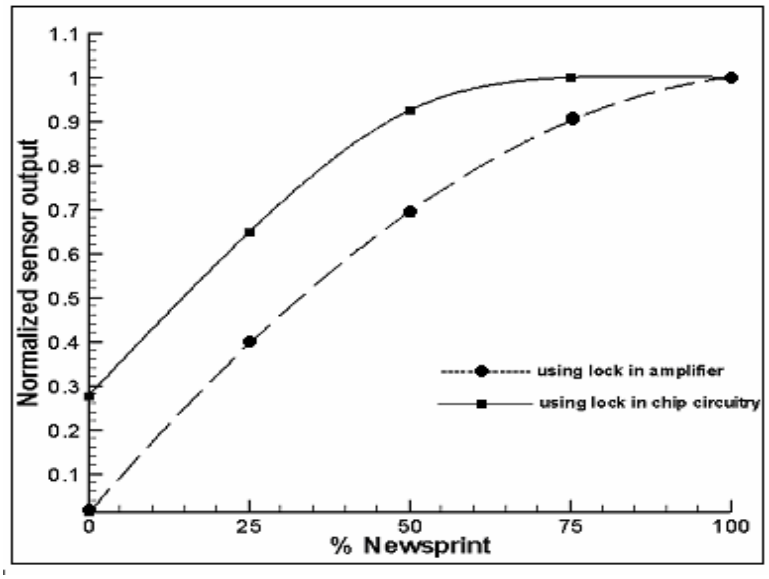

Figure 6.1.5. Comparison for MP – NPS blends

The above results show satisfactory performance of the lock in circuitry under static conditions, i.e., when the paper sample is not moving. Figure 6.1.6 illustrates the set up used to test the circuit under dynamic conditions.

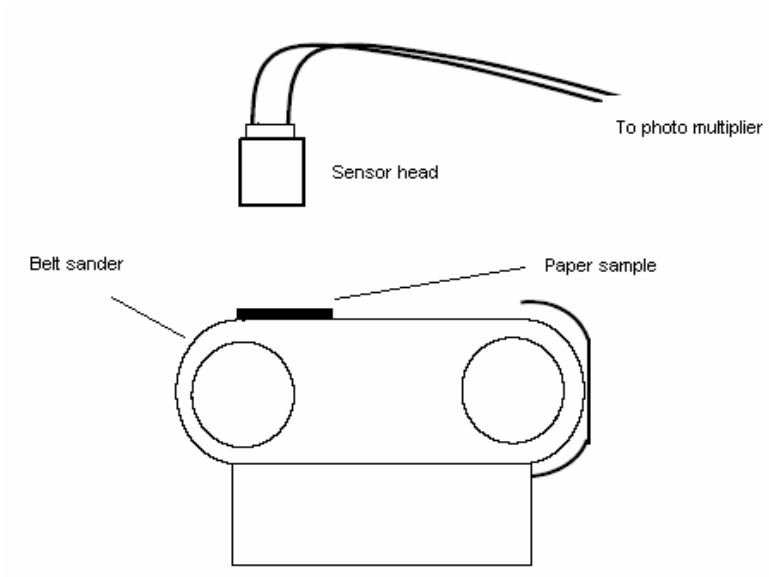

Figure 6.1.6. Dynamic test setup

A newsprint paper sample was pasted on the belt sander and the sensor head was placed 70 mm over the belt sander. The belt sander was run at varying speeds and it was found that the response of the sensor did not correctly indicate the lignin content in the paper sample due to overshoot and long response time of the circuit. Even at moderately high speeds the sensor response was poor.

6.2. Photon counting module

In order to overcome the disadvantages of the lock in circuit and to find a suitable replacement for the lock in amplifier, a photon counting module was considered. The photon counting module from Perkin Elmer is also called the Channel Photo multiplier DC module (MD962 with a spectral bandwidth from 165 – 850 nm). It essentially contains a channel photo multiplier, a high voltage power supply, an amplifier with I/U (current to voltage) conversion and an active quenching circuit for high light protection. It has exceptionally low noise and high sensitivity and hence facilitates detection of extremely low light levels.

Because of the high sensitivity and gain characteristics of the photon counting module, lock in amplification technique is not used for fluorescence intensity measurement. The MD962 module takes in the fluorescence and gives an output between 0 to 10 volts proportional to the intensity of fluorescence. This means that the laser light does not have to be chopped at 1500 Hz. A continuous source can be used for excitation. This eliminates the use of the chopper and chopper controller in the sensor setup.

One other advantage of using the photon counting module is that a low power diode laser (VLM-532-43LCC 15 mW, 532 nm from Quarton Inc) can be used instead of a 50 mW solid-state pumped diode laser. Comparable performance can be achieved with a low power laser by using the photon counting module at a high gain. Figure 6.2.1 shows the results obtained.

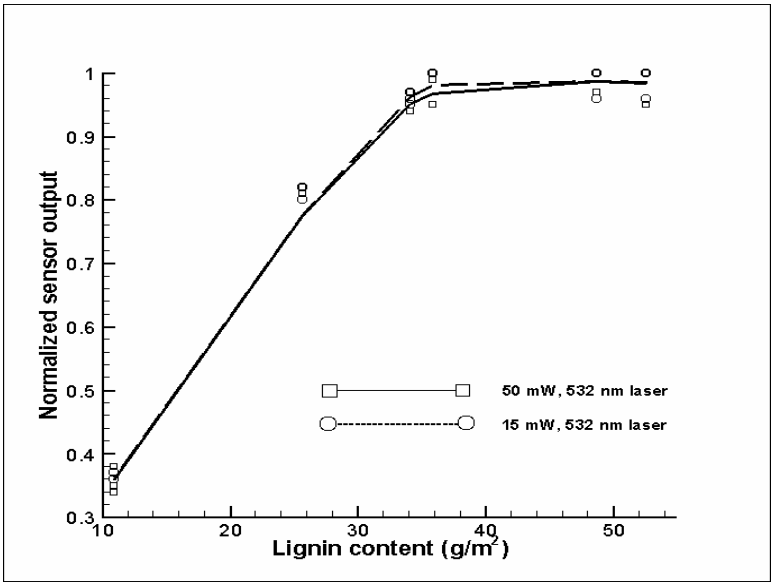

Figure 6.2.1. Laser performance comparison

Control voltage (0 – 3 volts, illustrated in figure 16.1.2) sets the current gain of the photon counting module. Figure 16.1.1 gives variation of current gain with control voltage. By using a 50 mW laser the MD962 module was operated at a control voltage of 1.073 volts. To get the same sensor characteristics using a 15 mW laser, the MD962 module was operated with a control voltage of 1.152 volts.

Figures 6.2.2 and 6.2.3 show the redesigned compact lignin sensor (from here on referred to as the new sensor) setup. The new sensor is more economic, less bulky, easily transportable and shows good performance characteristics.

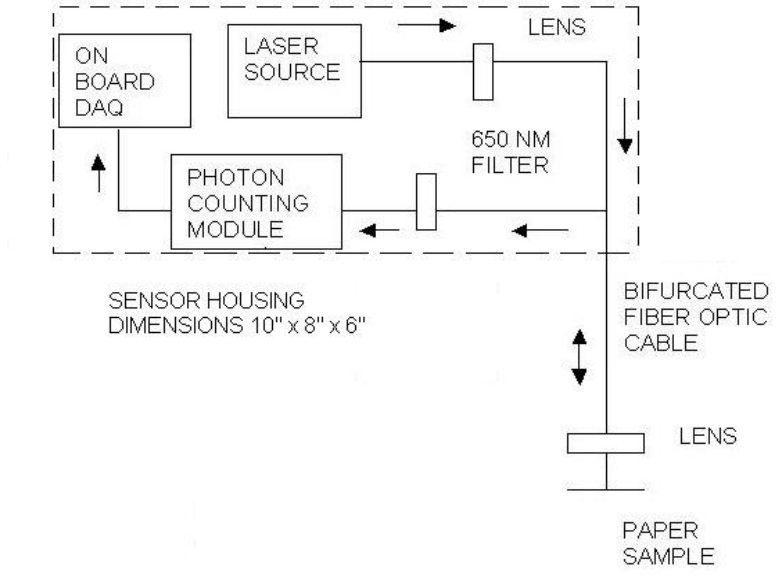

Figure 6.2.2. Redesigned lignin sensor schematic

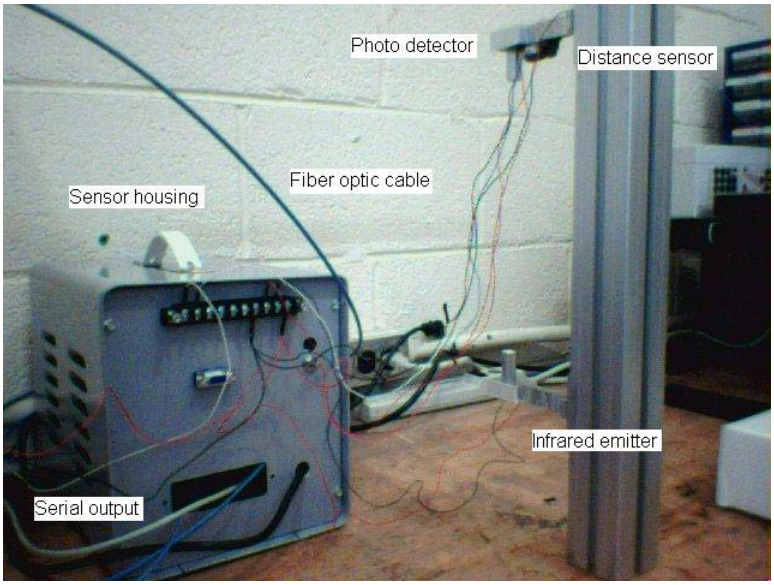

Figure 6.2.3. Redesigned lignin sensor

7. Dynamic performance comparison

Figure 7.1 [1] shows the dynamic response of the old sensor. Four samples (KP, TMP, WLP, NPS) were placed on a conveyor and the data was captured when the conveyor was moving at 720 feet per minute. The fluorescence intensity is represented in arbitrary units.

Figure 7.2 shows the dynamic response of the new sensor. Two samples (NPS and CP) were placed on the belt sander and the data was captured when the belt sander was run at 660 feet per minute.

From the graphs we see that the new sensor performs excellently under dynamic conditions. It gives accurate sensor output without any overshoot. It has a very short response time making it ideal for high-speed sorting of paper.

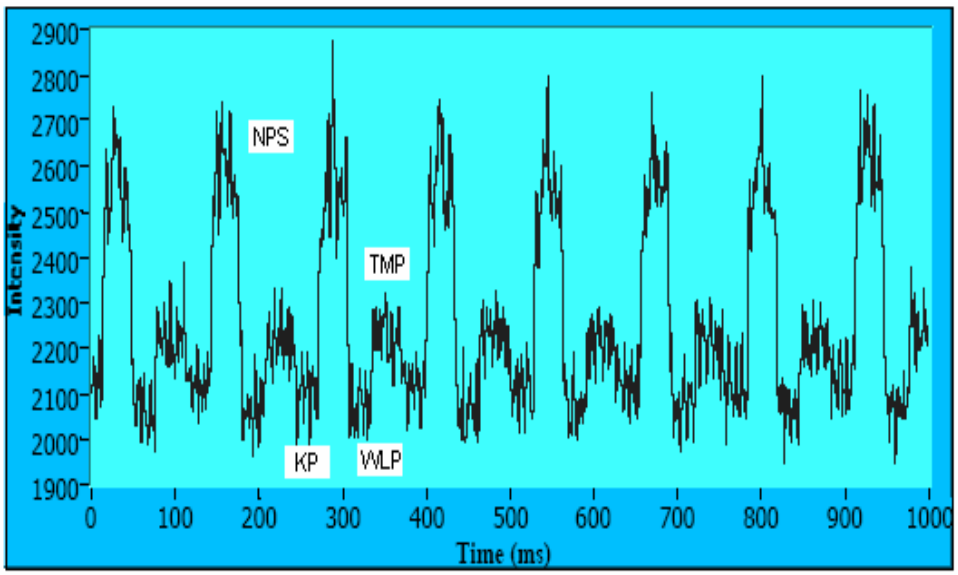

Figure 7.1. Dynamic response of old sensor [1]

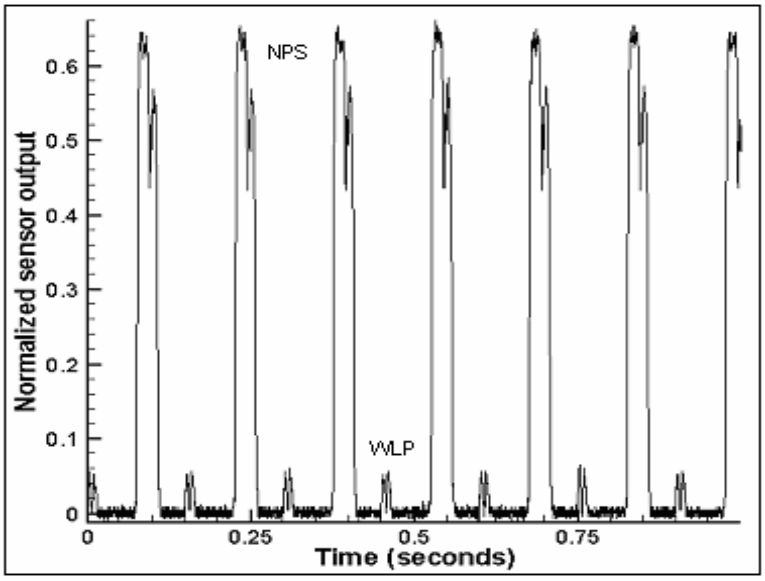

Figure 7.2. Dynamic response of new sensor

8. Red laser

To understand the effect of excitation wavelength on sensor response, a red laser source (635 nm) at the same power level (15 mW) was used. Fluorescence was picked up at 690 nm. Figure 16.4.3 gives the transmission spectrum of the filter used. The sensor response was compared with the results obtained using a green laser (532 nm). Figure 8.1 shows a comparison between the two results. While there is a correlation between the sensor output and lignin content in both cases, the green laser seems to have a higher initial slope and reaches saturation quickly. Sensor response using a red laser does not show any saturation.

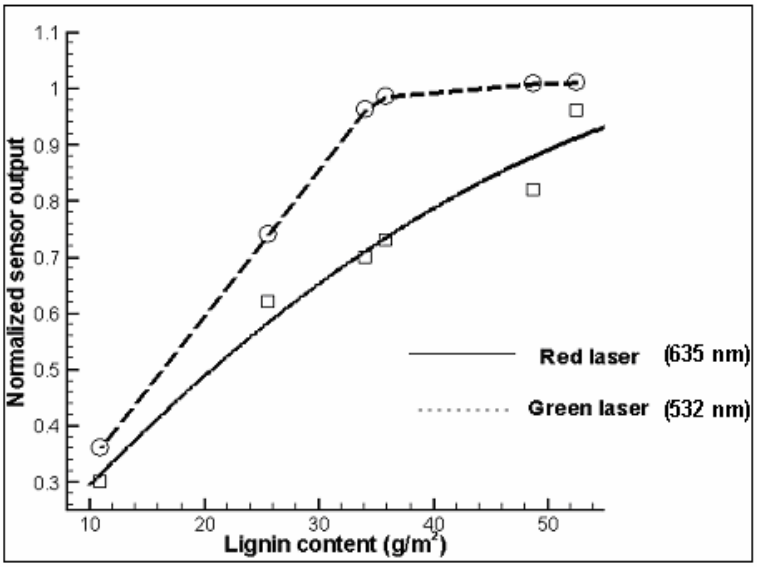

Figure 8.1. Performance of green and red lasers

The following equation relates the energy of the photons (in the laser) to the wavelength of the laser.

$$E = \frac{hc}{\lambda}$$

It is obvious from the equation that energy is inversely proportional to wavelength. Red laser (635 nm) has a higher wavelength than green (532 nm) and so energy of the individual photons is less in case of the red laser. Hence, sensor response does not show saturation using a red laser.

9. Effect of filter bandwidth

Figure 9.1 [1] shows the fluorescence spectrum obtained from newsprint and white ledger paper when excited with a green laser (532 nm).

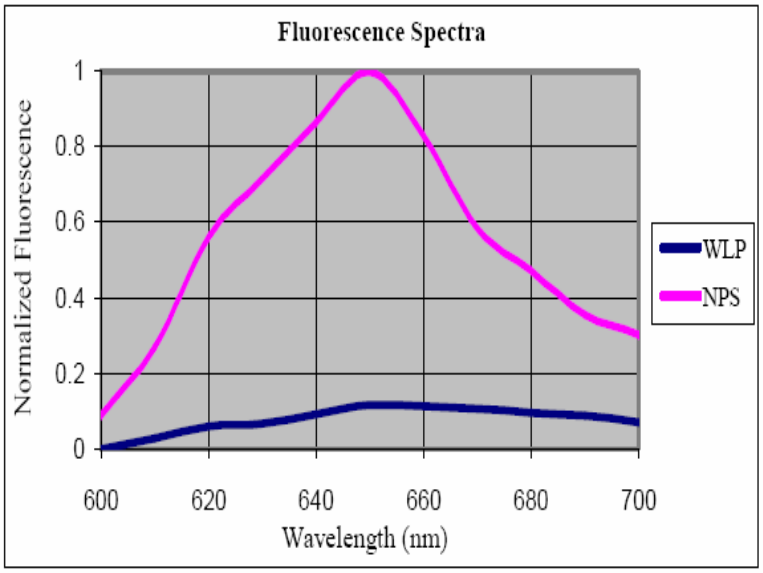

Figure 9.1. Fluorescence spectra [1]

From the figure it can be observed that the fluorescence peak is at 650 nm. There are two ways to measure the intensity of fluorescence. The first method is to use a filter which has a narrow bandwidth, centered at 650 nm (from hereon referred to as the narrow filter). The second method [4] is to use a filter, which has a broad bandwidth, centered at 650 nm (from hereon referred to as the broad filter). In the first method, only the intensity of fluorescence peak is measured whereas in the second method, fluorescence response is integrated over a wider wavelength range.

All the experiments described above use a narrow filter, 03FIL252 (purchased from Melles Griot). The bandwidth of the filter is 650 +/- 10 nm. Experiments were done using a broad filter (03FIB314) to compare the performance of the sensor. The broad filter has a bandwidth of 650 +/- 50 nm. Figures 16.4.2 and 16.4.4 give the transmission spectra of the filters.

Figures 9.2, 9.3 and 9.4 show the results obtained using hand sheet samples made from NPS, CP – NPS blends and MP – NPS blends.

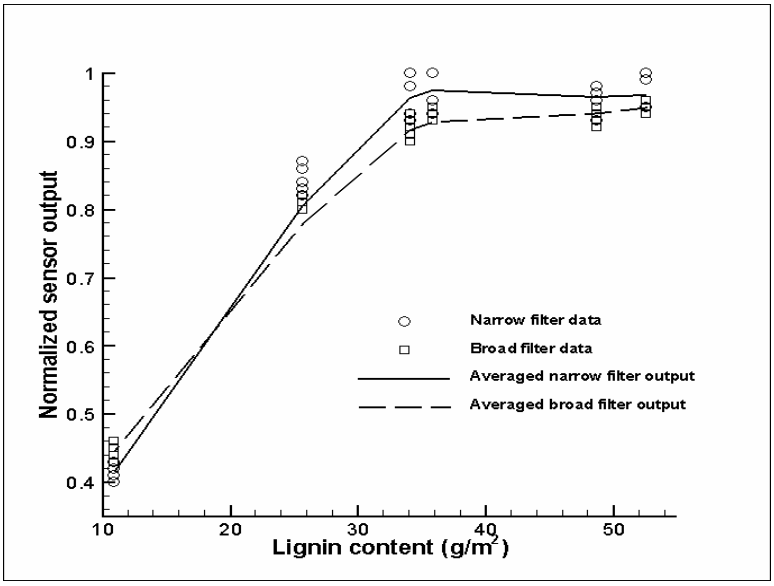

Figure 9.2. Filter comparison for NPS samples

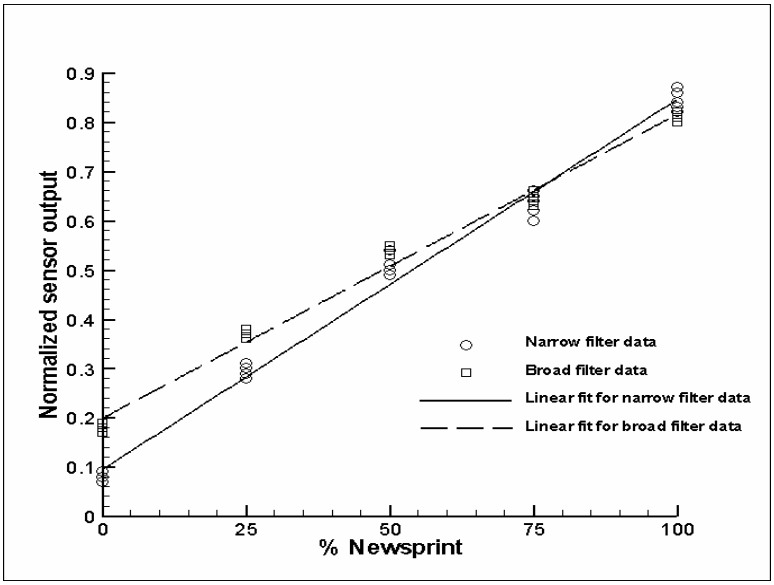

Figure 9.3. Filter comparison for CP blends

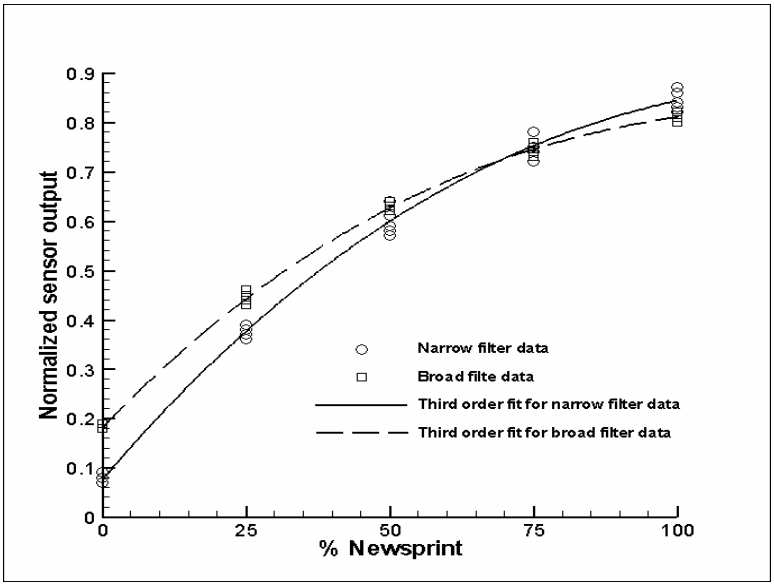

Figure 9.4. Filter comparison for MP blends

From the above graphs it is observed that the sensor response shows more gradient (higher slope) using a narrow filter than a broad filter. Hence a narrow filter is better suited for paper sorting applications.

10. Effect of color

10.1. Theory

This section discusses the effect of color on sensor response. Particularly, effect of color printed on the paper is considered, rather than color of the paper itself. This is because colored paper is sorted using a color tracking system. Paper samples with localized areas of printed color could be sorted as newsprint or colored paper depending on the amount of color and lignin. Hence, the effect of printed color on lignin sensor response is considered in this section. All the experiments in this section were done using a green laser. There are three key factors that affect the sensor response (apart from lignin content). They are:

1. Transmittance of the color at excitation wavelength (532 nm)
2. Transmittance of the color in the fluorescence bandwidth (650 +/- 10 nm)
3. Printed color dye fluorescence

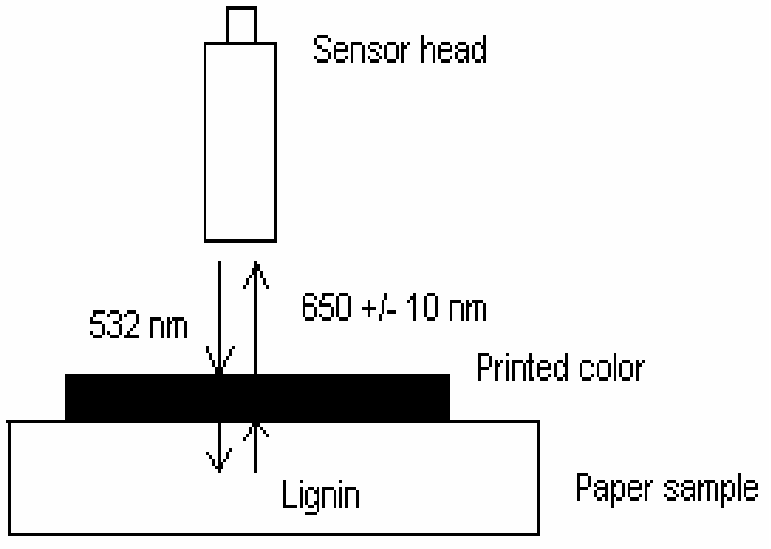

Figure 10.1.1. Effect of color

Transmittance of a layer is defined as the ratio of the transmitted intensity to the incident intensity of light. Hence, if a layer has high transmittance, it transmits most of the energy incident upon it.

The intensity of fluorescence depends upon the transmittance of the color at the excitation wavelength. If the color has high transmittance at 532 nm (excitation wavelength) then most of the energy will be transmitted to the lignin molecules underneath it, thus resulting in a potentially higher fluorescence. Figure 10.1.1 illustrates this concept.

Similarly, the intensity of fluorescence picked up by the sensor depends on the transmittance of the color in the fluorescence bandwidth (650 +/- 10 nm). If the printed color layer has high transmittance in this bandwidth then most of the fluorescence will be detected by the sensor, thus resulting in high sensor response. If the printed color has low transmittance in this bandwidth, then even though there is high lignin content in the paper, the fluorescent light cannot pass through the color to the sensor.

Some of the dyes used for color printing use fluorescing agents, to make the color look brighter. So, if the printed color uses such fluorescent dyes then the sensor response will be confounded and not uniquely related to lignin content in paper.

10.2. Experiments and results

Different colors were printed on CP using a HP Desk jet 820 Cse color printer. The color samples are shown in appendix 16.5. These samples were placed under the lignin sensor and the response was noted (Table 10.2.1). The numbers 1 and 2 in the color description indicate two different shades of the same color. Copy paper does not contain any fluorescence, so a high sensor response indicates the presence of fluorescing agents in the color.

Table 10.2.1 Color data

Color on CP	Description	L*	a*	b*	Normalized sensor output
11A	Maroon	45.2	35.6	12.6	0.48
11B	Light maroon	54.4	33.5	29.2	0.9
11C	Red	52.4	41.7	21.5	0.81
11D	Light red	57.4	36.7	15.1	0.5
12A	Dark green 1	50.4	-32.7	22.8	0.07
12B	Green 1	63.9	-38.3	30	0.08
12C	Bright green 1	67.9	-34.6	22.6	0.09
12D	Brighter green 1	74.2	-25.9	16.8	0.11
13A	Dark blue 1	43.2	7.3	-33.9	0.12
13B	Blue 1	52.5	-1	-33.6	0.09
13C	Bright blue 1	56.7	-7.5	-32.8	0.08
13D	Brighter blue1	77.6	-13.4	-17.1	0.1
14A	Dark yellow	77.3	12.1	67.2	0.8
14B	Yellow	85.3	2.1	79.4	0.24
14C	Bright yellow	89.9	-2.2	30	0.2
14D	Brighter yellow	91.6	-1.1	12.8	0.2
15A	Black	33.9	1.7	1.7	0.04
15B	Grey	64.2	0.6	0.7	0.07
15C	Light grey	74.9	0.4	0.4	0.11
15D	Lighter grey	83.5	0.2	0.1	0.14
16A	Dark red	40.3	28.3	13.4	0.38
16B	Pink	52.8	45.7	-12.8	0.26
16C	Orange	62.5	31.6	44.3	1
16D	Light orange	70.2	22	7.7	0.28
17A	Purple	44.8	42.5	-17.8	0.29
17B	Light purple	47.7	50.6	-13.1	0.32
17C	Brown	65.5	10.3	49.8	0.46
17D	Dark brown	54.9	9.2	18.4	0.21
18A	Dark blue 2	40.7	21.2	-29.5	0.24
18B	Blue 2	54.4	13.7	-28.1	0.1
18C	Light blue 2	66.1	0.7	-23.4	0.12
19A	Dark cyan	52.9	-22.7	-18	0.04
19B	Cyan	70.1	-29.4	-15.9	0.07
19C	Light cyan	65.3	-29.9	-31.3	0.05
20A	Dark green 2	74	0	61.3	0.14
20B	Green 2	80.1	-13.5	54.6	0.17
20C	Light green 2	82.3	-13.7	25.2	0.15

It can be seen from table 10.2.1 that colors 11A, 11B, 11C, 11D, 14A, 16A, 16C, 17B and 17C show a sensor response greater than 0.3. Copy paper alone without any color

gives a sensor response less than 0.1. Hence, it can be concluded that these colors have fluorescent dyes. To further confirm this result the following experiment was performed.

The fluorescing samples 11A, 11C, 14A and 16C were printed on HP premium inkjet transparency film (HP C3834A). Figure 10.2.1 shows the experimental setup.

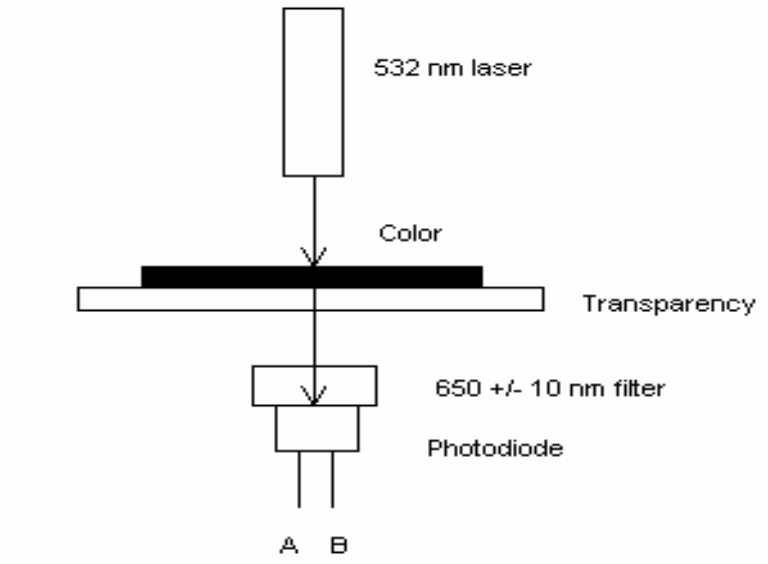

Figure 10.2.1. Dye fluorescence

Laser light is focused on the color sample printed on a transparency. The fluorescence, if any, is picked up by the photodiode (Hamamatsu, S2386-45K) after passing through the filter. The filter does not transmit 532 nm, hence the photodiode picks up only fluorescence. Figure 16.6.1 shows the spectral response of the photodiode. The experiment is done in darkness to make sure that the photodiode responds only to fluorescence and not to stray light. The output is measured as short circuit current across terminals A and B of the photodiode. Table 10.2.2 shows the results obtained.

Table 10.2.2. Dye fluorescence data

Sample	Description	L*	a*	b*	Diode output
Laser with 650 nm narrow filter	No color				0.06 microamps
Clear transparency	No color				0.05 mircoamps
11C	Red	52.4	41.7	21.5	0.11 microamps
11A	Maroon	45.2	35.6	12.6	0.09 microamps
14A	Dark yellow	77.3	12.1	67.2	0.15 microamps
16C	Orange	62.5	31.6	44.3	0.17 microamps

From the Table 10.2.2 it is observed that the output for the color samples is two or three times greater than the output for a clear transparency. This result confirms the hypothesis that the dyes in these color samples are indeed fluorescent.

The following experiment was performed to determine the effect of the transmittance of the color on the sensor response. Color samples, which did not show any fluorescence, were printed on a transparency and the transmittance of these samples was determined using the set up shown in figures 10.2.2 and 10.2.3.

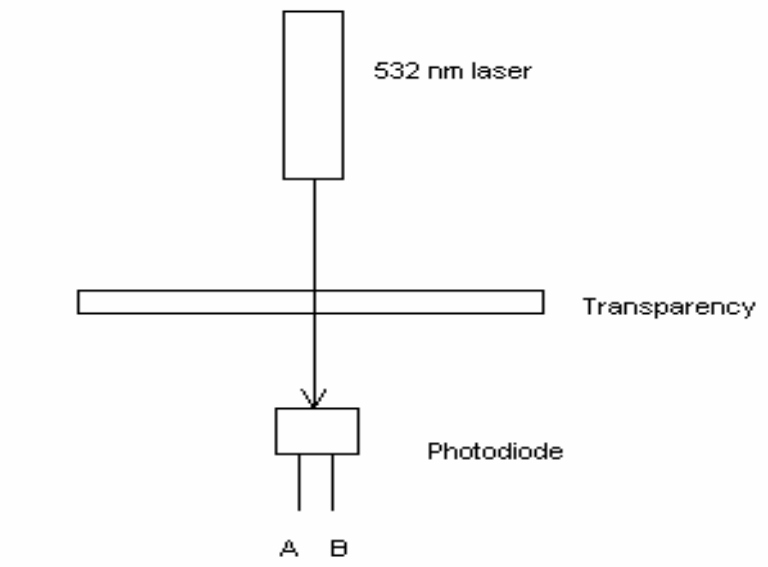

Figure 10.2.2. Incident intensity measurement

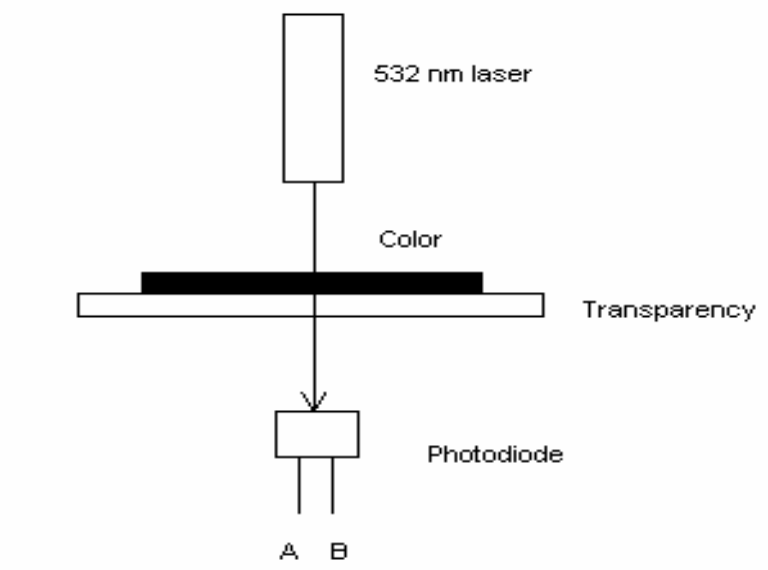

Figure 10.2.3. Transmitted intensity measurement

Figures 10.2.2 and 10.2.3 show the set ups used for measuring the incident intensity and transmitted intensity of light, respectively. The ratio of transmitted to incident intensity gives the transmittance of the color sample. The color samples used for this experiment were 12A, 12B, 12C, 12D, 13A, 13B, 13C, 13D, 15A, 15B, 15C, 17A, 17B, 17D, 18A, 18B, 18C, 19A, 19B and 19C. These samples were printed on newsprint and the sensor response was acquired. Figure 10.2.4 gives the plot of sensor response vs. transmittance of 532 nm.

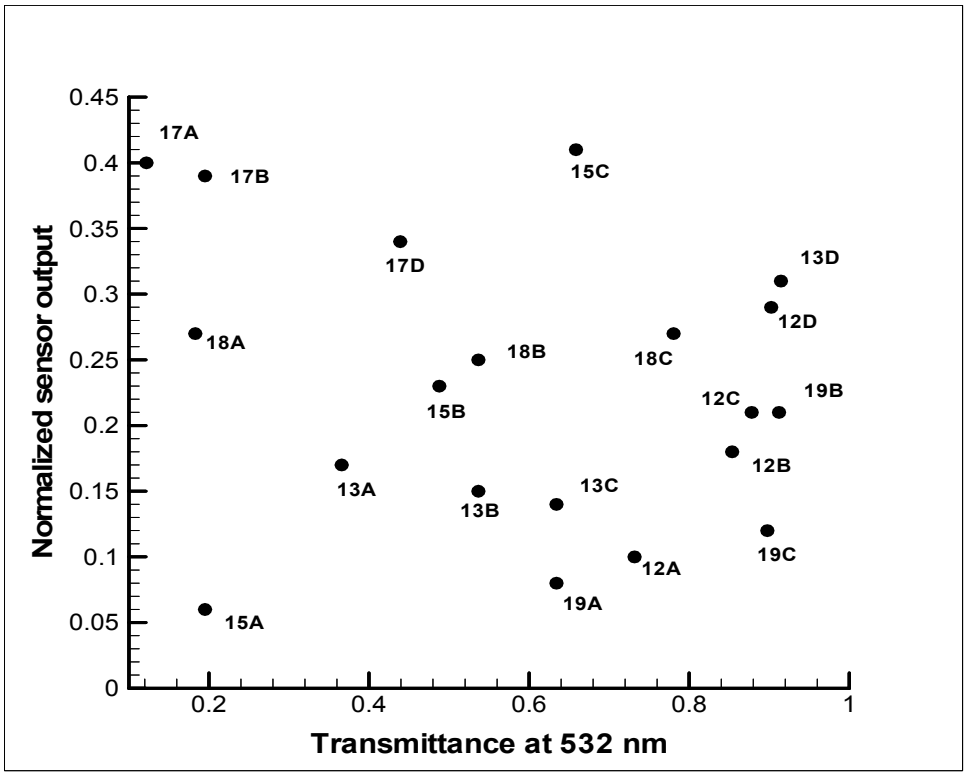

Figure 10.2.4. Effect of laser transmittance

From figure 10.2.4 it can be observed that there is no clear correlation between sensor output and transmittance of the printed color at the excitation wavelength. Newsprint without any color gives a normalized sensor output between 0.4 and 0.5. Even at relatively low transmittances, there are colors for which the sensor shows true lignin content. This indicates that even at low transmittances, there is enough energy available for the lignin molecules to fluoresce. This shows that the transmittance of the laser is not a critical factor affecting the sensor response. We can also observe from figure 10.2.4 that even at relatively high transmittance values, some samples show less sensor response. This also indicates that the transmittance of printed colors at 532 nm is not a crucial factor affecting the sensor response. It is hypothesized that the transmittance at 650 nm is the critical factor affecting the sensor response with printed color samples.

To test this hypothesis, transmittance of the color samples at 635 nm was determined using the set up shown in figures 10.2.2 and 10.2.3. Ideally, transmittance at 650 nm would have to be determined, but due to the absence of a 650 nm laser and the

availability of a 635 nm laser, this experiment was done. It is assumed that the transmittances at 650 and 635 nm would be comparable. Figure 10.2.5 shows the plot of sensor response vs. transmittance at 635 nm.

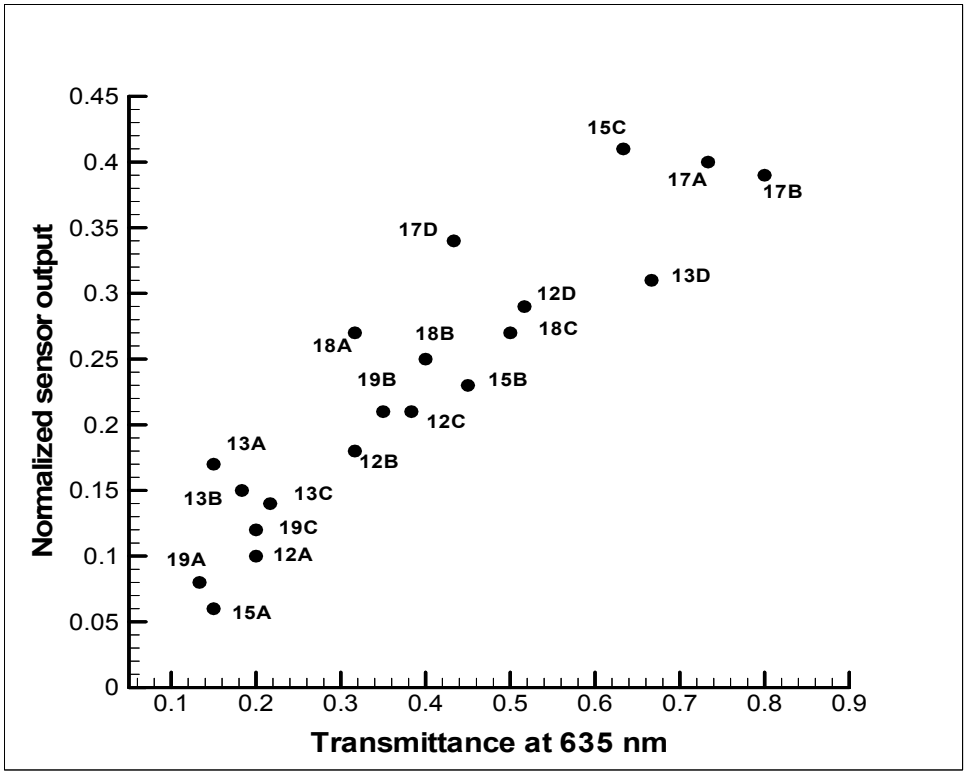

Figure 10.2.5. Effect of transmittance at 635 nm

From figure 10.2.5 it can be observed that the transmittance in the fluorescence bandwidth (around 650 nm, in this case 635 nm) has a strong correlation with the sensor output. The graph shows a linear response with some scatter. As transmittance increases, more fluorescence goes through the color layer and is picked up the sensor.

10.3. Photon calculation

It is postulated that the dependence of the sensor to fluorescence and not incident intensity is due to the fluorescence intensity being much less than the incident intensity. The following shows the calculation of the ratio of excitation photons to fluorescence photons.

Calculation for number of photons emitted by laser (635 nm) in one second:

Energy of one photon, $E_o = \frac{hc}{\lambda} = \frac{6.63*10^{-34}*3*10^{8}}{635*10^{-9}} = 3.13*10^{-19} Joules$

Power of laser, $P = 15mW$

Energy delivered in one second, $E_t = P*t = 15*10^{-3} Joules$

Number of photons emitted, $N_0 = \frac{E_t}{E_o} = \frac{15*10^{-3}}{3.13*10^{-19}} = 4.79*10^{16}$

Calculation for number of photons emitted due to fluorescence in one second:

Current to voltage conversion factor for photon counting module, $I_{cv} = 0.01v/nA$

Anode current for 10 volts output, $I_a = \frac{10}{0.01} nA = 1000nA$

From figure 16.1.1, current amplification at a gain control voltage of 1.4 Volts, $g = 10^5$

Hence cathode current, $I_c = \frac{I_a}{g} = \frac{1000}{10^5} = 10^{-11} A$

Number of electrons emitted by cathode per second, $N_c = N*I_c = 6.24*10^{18}*10^{-11}$

Hence, $N_c = 6.24*10^7$

Quantum efficiency (QE) of a photo multiplier tube is defined as the ratio between the number of electrons emitted by the photo cathode to the number of incident photons.

From figure 16.1.2 QE for MD 962 module is 4%. So, QE = 0.04.

Hence, number of photons incident on the cathode, $N_{cat} = \frac{N_c}{QE} = \frac{6.24*10^7}{0.04}$

Hence, $N_{cat} = 156*10^7$

From figure 16.4.3, peak transmittance of optical filter is 75%. So, t =0.75.

Hence, number of photons emitted due to fluorescence, $N_f = \frac{Ncat}{t} = \frac{156*10^7}{0.75}$

Therefore, $N_f = 208*10^7$

Ratio of number of excitation photons to fluorescence photons, $r = \frac{N_o}{N_f} = 2.3*10^7$

10.4. Results

From the photon calculation, we can observe that the number of excitation photons is far greater than the number of photons emitted due to fluorescence. Hence the printed color transmittance of light at the fluorescence wavelength is a far more critical factor than the transmittance at the excitation wavelength.

From the data obtained, we can conclude that the sensor is not capable of predicting lignin content accurately for color printed samples. Dye fluorescence and transmittance of the color are two key factors affecting sensor response.

For high speed sorting applications, the lignin sensor will not be able to detect lignin in papers printed completely with color. However, for paper with partial coverage, if the lignin sensor is capable of making several measurements on a single paper, an algorithm that chooses the maximum (or other suitable statistical descriptor) signal reading for the paper could be used to detect lignin.

11. Effect of distance between paper sample and sensor

11.1. Initial results

Figure 11.1.1 [1] shows the effect of distance on fluorescence intensity. From the graph it can be observed that fluorescence picked up by the sensor drops drastically with distance. Hence to use the sensor for sorting paper, all the paper samples should be at the same distance from the sensor.

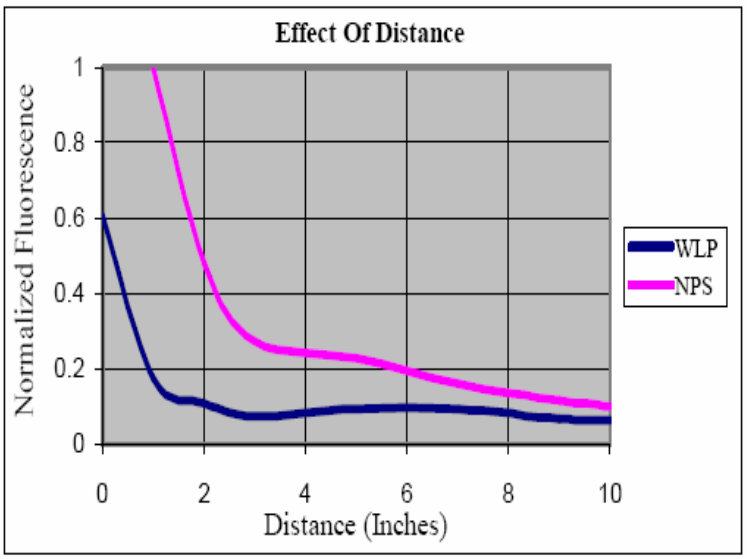

Figure 11.1.1. Effect of distance [1]

Figures 11.1.2 illustrates the situation where a stack of white ledger paper passes very close to the sensor. Figure 11.1.3 shows the situation where newsprint passes under the sensor at a distance of 2 inches. From figure 11.1.1 it can be observed that both these situations give the same sensor response. In a commercial sorting facility, it is difficult to make sure that all the samples pass at the same distance from the sensor. Hence to distinguish between newsprint and white ledger paper, the sensor response needs to be adjusted for varying distances.

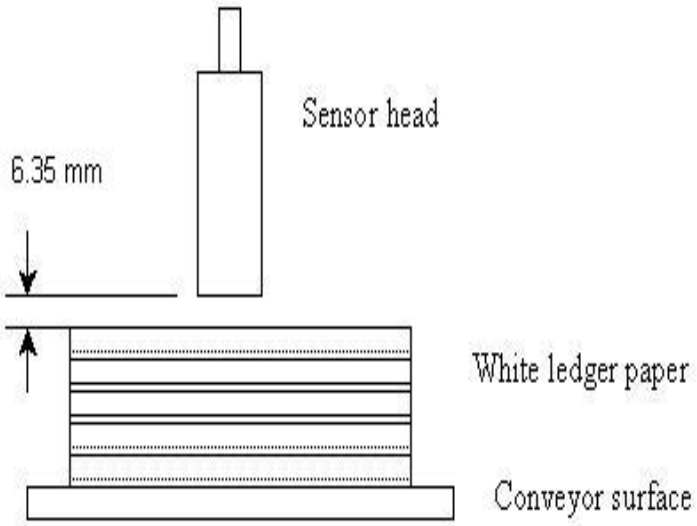

Figure 11.1.2. WLP under sensor

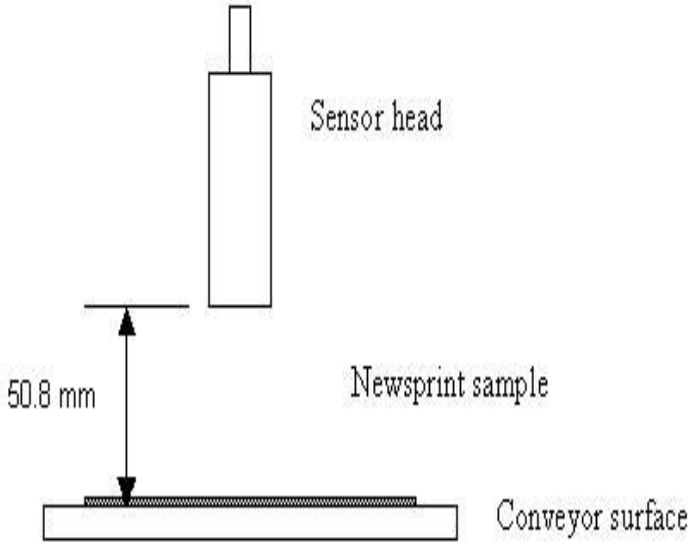

Figure 11.1.3. NPS under sensor

Figures 11.1.4 and 11.1.5 show the variation of sensor output with distance using green (excitation at 532 nm and fluorescence at 650 nm) and red (excitation at 635 nm and fluorescence at 690 nm) lasers. Different paper samples with varying lignin content were

used for the experiment. The sensor is calibrated so that a 4-gram hand sheet containing 100% newsprint would give the maximum output 1 inch (25.4 mm) from the sensor.

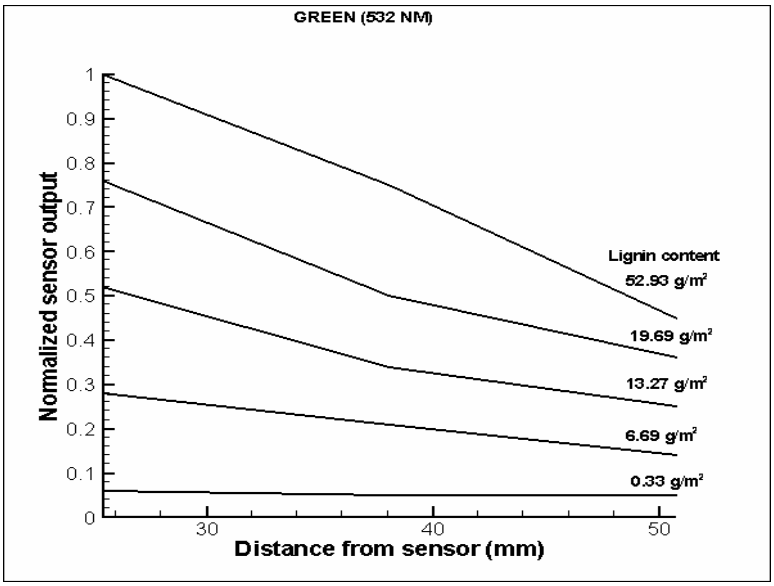

Figure 11.1.4. Effect of distance using green laser

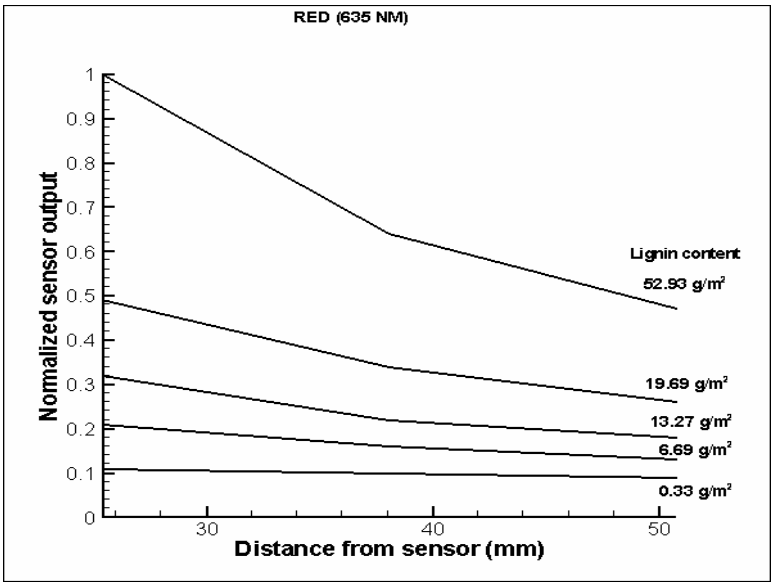

Figure 11.1.5. Effect of distance using red laser

It can be observed from figures 11.1.4 and 11.1.5, that a low lignin sample closer to the sensor gives the same (or higher) sensor output as a high lignin sample farther from the sensor. So, to differentiate between the two samples we need to know the sensor output at a standard distance from the sensor.

11.2. Distance correction

As mentioned earlier, the sensor is calibrated so that a 4-gram hand sheet containing 100% newsprint would give the maximum output 1 inch (25.4 mm) from the sensor. In actual operation, the sensor is placed at a height of 2 inches (50.8mm) from the conveyor. Figure 11.2.1 illustrates this concept. Distance sensor (Sharp, GP2D120) is used to measure the distance from the lignin sensor to the paper sample. Table 16.7.1 and figure 16.7.1 show the characteristics of the distance sensor.

By measuring the distance and the lignin sensor response and using a correction equation, we can predict the lignin sensor response at a standard distance. The standard distance is arbitrarily fixed at 1 inch (25.4 mm). The corrected sensor output at this distance is used for sorting paper. By using this method all the paper samples do not have to be presented at the same distance to the sensor.

In actual operation, if a paper sample comes closer than 1 inch to the sensor, its corrected value at the standard distance cannot be accurately predicted. Hence, this region (as shown in figure 11.2.1) is called the uncalibrated zone. If a paper sample comes in this region, then the sensor head would have to be moved up by an inch to predict its corrected value at the standard distance.

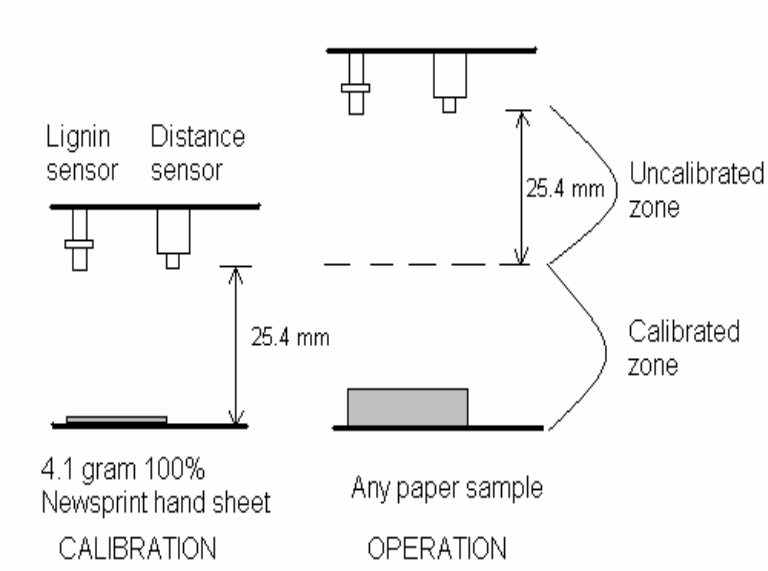

Figure 11.2.1. Sensor calibration and operation

If a paper sample comes between 1 and 2 inches to the sensor, its corrected value at the standard distance can be accurately predicted using a correction equation. Hence, this region (as shown in figure 11.2.1) is called the calibrated zone. If a paper sample comes in this region, then it can be accurately sorted, irrespective of its distance from the sensor head.

We observe from figures 11.1.4 and 11.1.5 that the sensor response "flattens" out as lignin content decreases. In other words, there is more variation in sensor response with distance for higher lignin content. Hence, to reasonably predict the sensor output at the standard distance (1 inch) we need a correction equation, which describes a surface with distance (in mm) on X-axis, lignin content (in g/m^2) on Y-axis and normalized sensor output on Z-axis.

11.3. Surface plots

Normalized sensor output from different paper samples (NPS, CP – NP blends and MP – NP blends with varying lignin content) was taken at different heights (between 1 and 2 inches) using green and red lasers. The data was plotted in 3D graphs as shown in figures 11.3.1, 11.3.2 and 11.3.3.

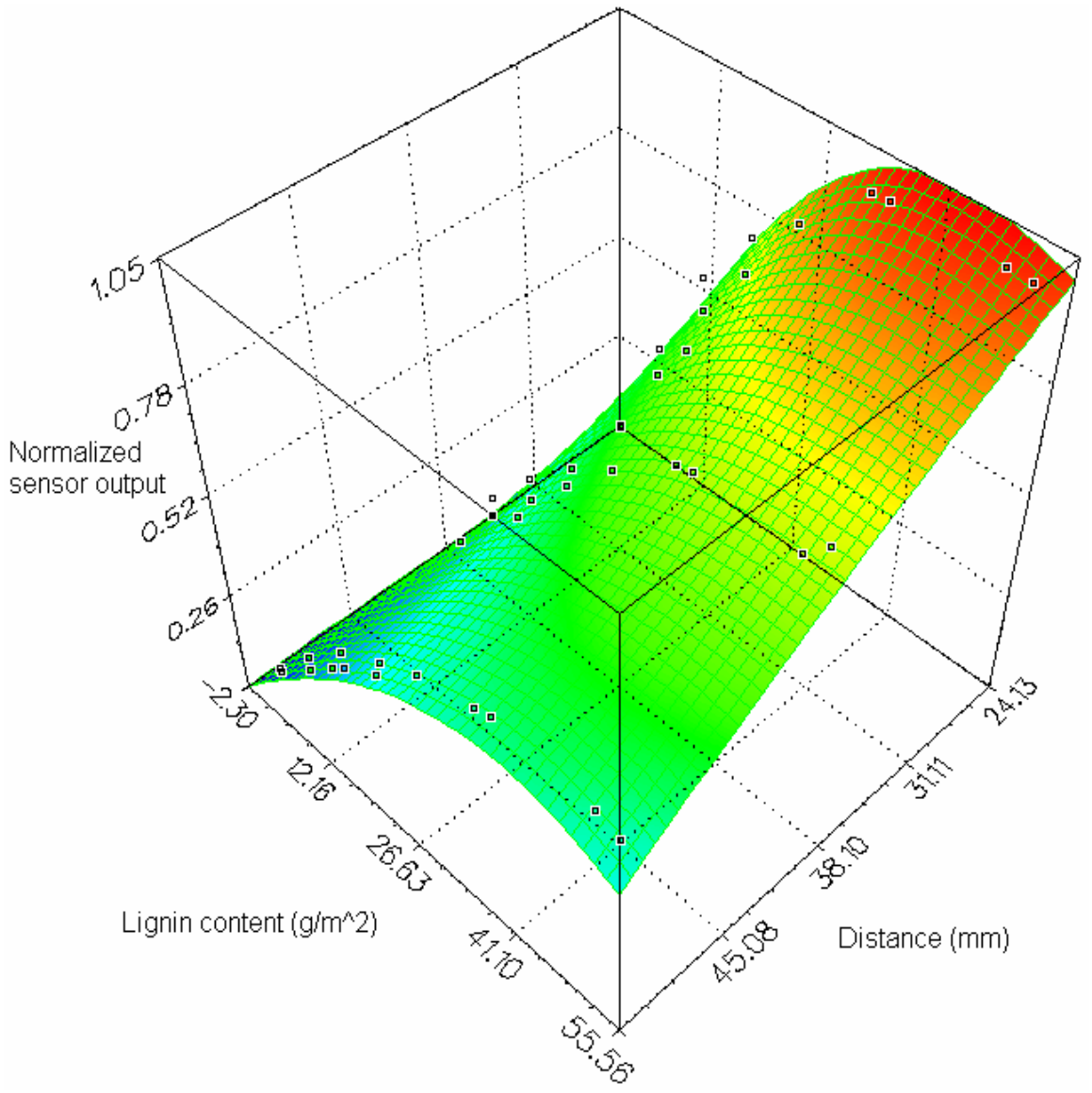

Figure 11.3.1. Correction surface I

Figure 11.3.1 shows a correction surface, which is a polynomial function with fourth order in Y and second order in X. The data points are obtained using a green laser.

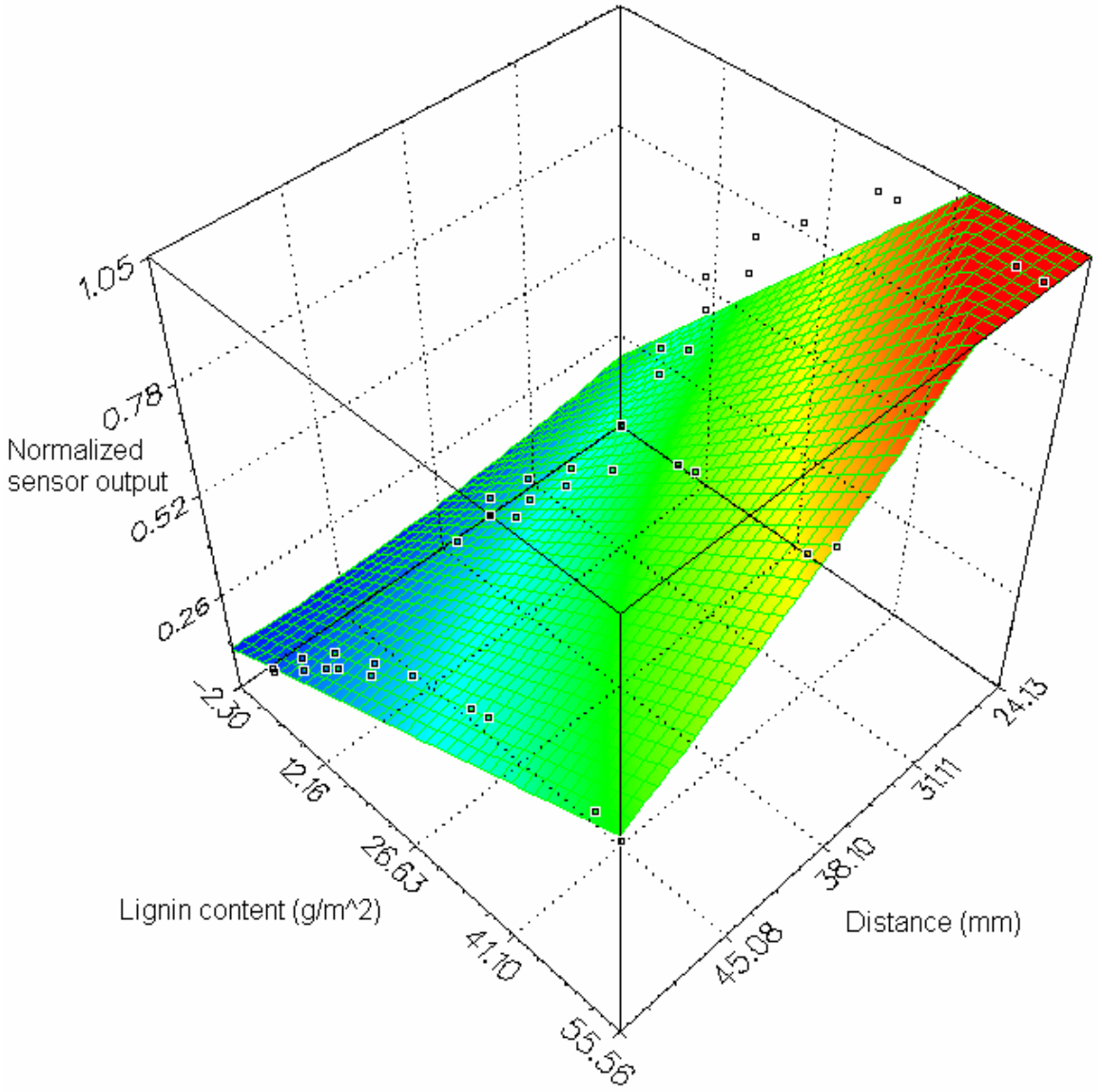

Figure 11.3.2. Correction surface II

Figure 11.3.2 and 11.3.3 show correction surfaces, which are polynomial functions with first order in Y and second order in X. Surface II and III are obtained using green and red laser respectively.

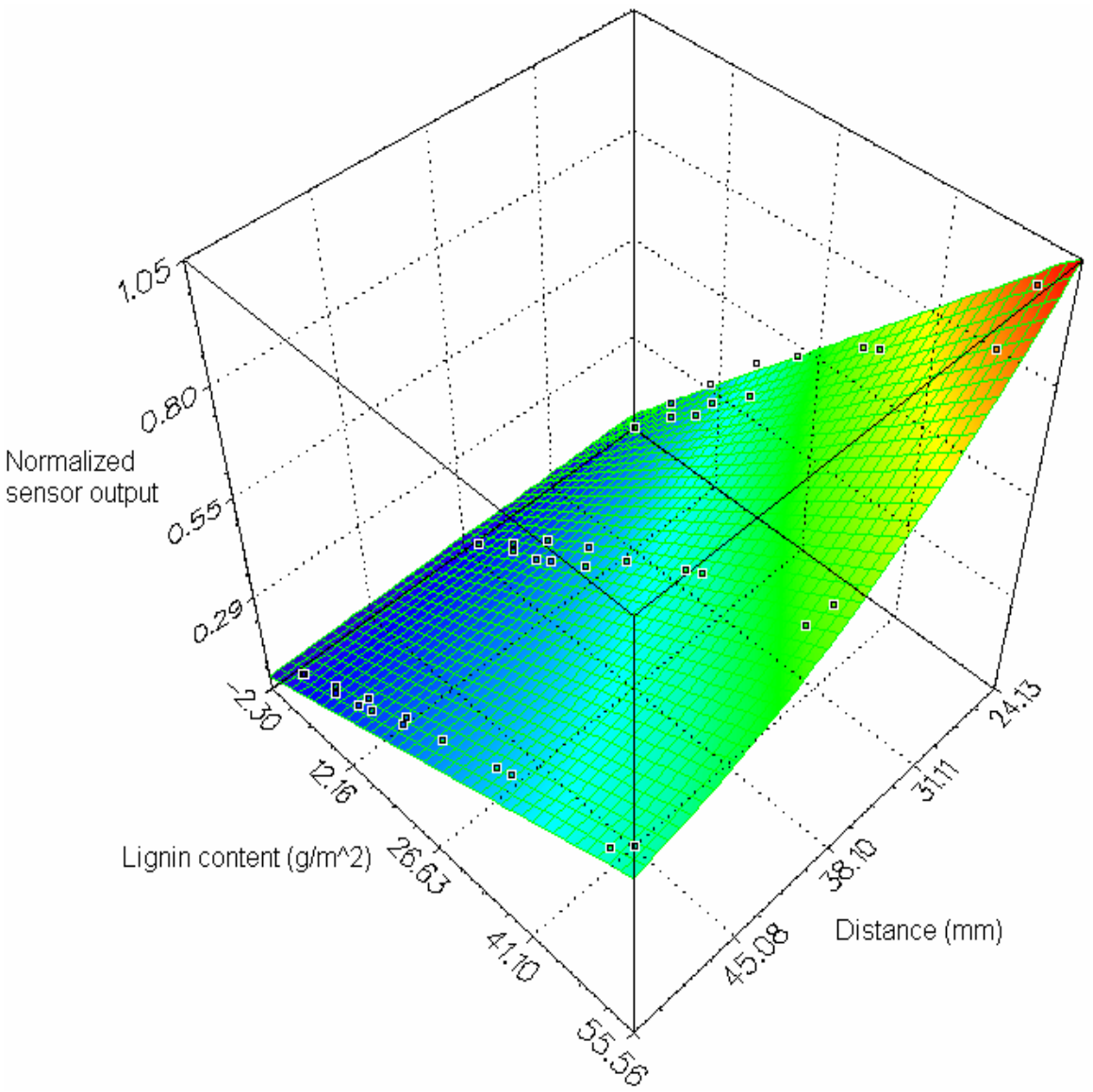

Figure 11.3.3. Correction surface III

It can be observed from figures 11.3.1 and 11.3.2, that correction surfaces using a green laser show saturation (red region in the graph). Figure 11.3.3 (using a red laser) shows a smoother correction surface without any saturation.

11.4. Results

Sensor response at 2 inches was used in the equations for correction surfaces I and II (using green laser) and the sensor output at 1.5 inches and 1 inch (standard distance) was predicted. Figure 11.4.1 shows the results obtained.

It can be observed from figure 11.4.1 that using a higher order equation (correction surface I) gives a better prediction than using a lower order equation (correction surface II). Since using a higher order equation requires more computation time, this would not be very easy to use for high speed sorting applications.

Figure 11.4.2 shows the results obtained using correction surface III (for a red laser). It can be observed from the graph that the predicted values match the actual values very closely by using a lower order equation. This indicates that a red laser would be better suited for distance correction.

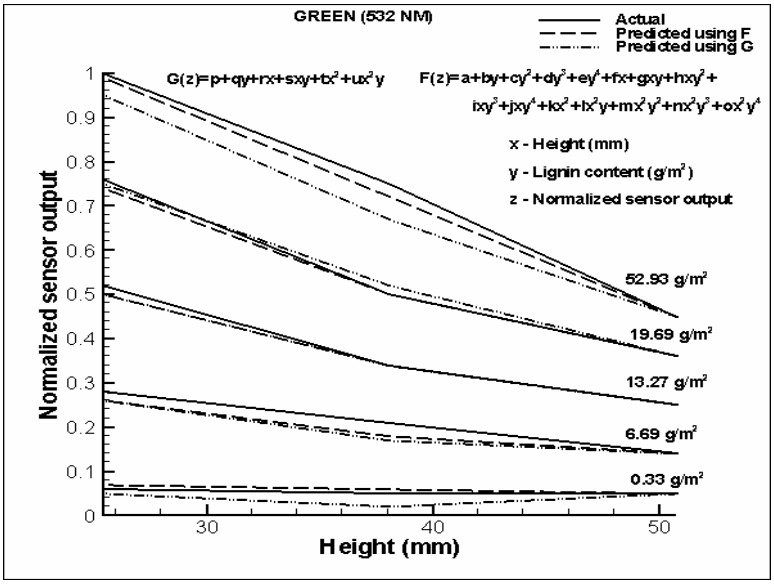

Figure 11.4.1. Distance correction plot for green laser

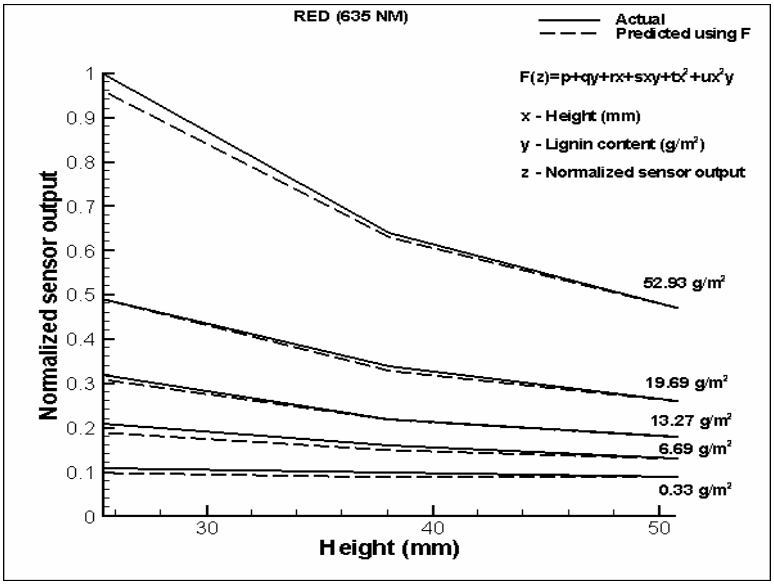

Figure 11.4.2. Distance correction plot for red laser

12. Solenoid system

12.1. Solenoid model design

From figure 11.2.1 it can be seen that if a paper sample comes within 1 inch of the sensor head, then the sensor response cannot be corrected for distance. In such cases the sensor head and the distance sensor would have to be moved up by an inch for distance correction. This is accomplished by using cascaded solenoids. Figure 12.1.1 shows a schematic of the solenoid system.

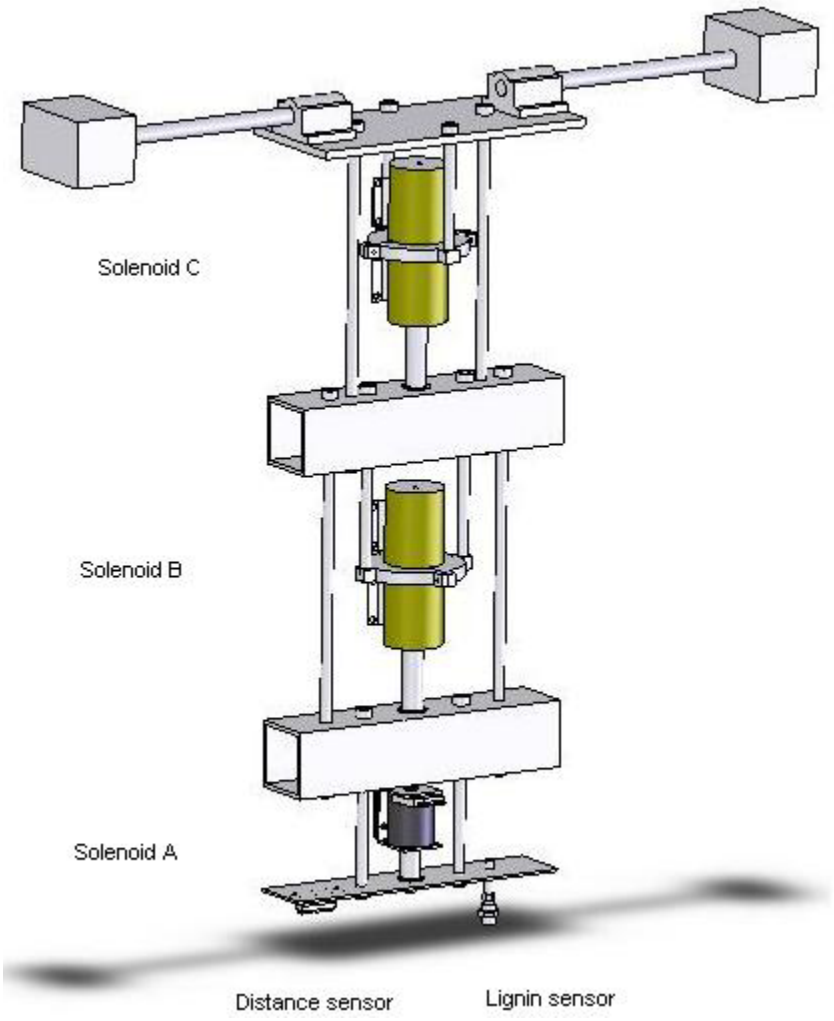

Figure 12.1.1. Solenoid model

Solenoid A (Saia Burgess, C34-273-M-33) has a stroke of 1 inch. Solenoids B and C (Saia Burgess, 194580-25) have a stroke of 2 inches. All three solenoids are pull type, i.e., when energized the plunger is pulled into the solenoid. The specifications, performance characteristics, force and response time data for the solenoids are given in section 16.8. Figure 12.1.2 shows a snapshot of the actual solenoid system.

Figure 12.1.2. Solenoid system

By firing the three solenoids in different combinations the sensors can be moved up by 5 inches in steps of an inch. Table 12.1.1 shows the firing combinations.

Table 12.1.1. Solenoid firing combinations

Distance moved in inches	Solenoid combinations
0	None
1	A only
2	C only
3	A and C
4	B and C
5	A, B and C

The solenoids are fired using solenoid driver circuits. The output of the drivers can be enabled with a logic signal.

12.2. Time response curves

Time response curves are obtained by giving a step input (logic enable to the solenoid circuit) and measuring the distance (using a sharp GP2D12 sensor) moved by the solenoid plunger as a function of time. Figure 12.2.1 shows the time response curve of solenoid A.

It can be observed from figure 16.7.3 that the measurement time of the distance sensor is typically 40 ms. Hence, from figure 12.2.1 we can infer that the solenoid takes less than 40 ms to move one inch.

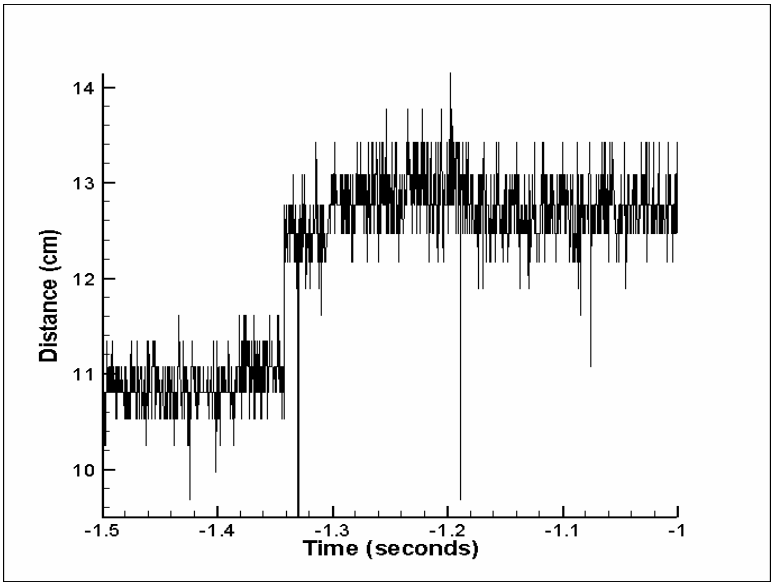

Figure 12.2.1. Time response of solenoid A

Figure 12.2.2 shows the time response of solenoid C. The solenoid takes less than 200 ms to move 2 inches.

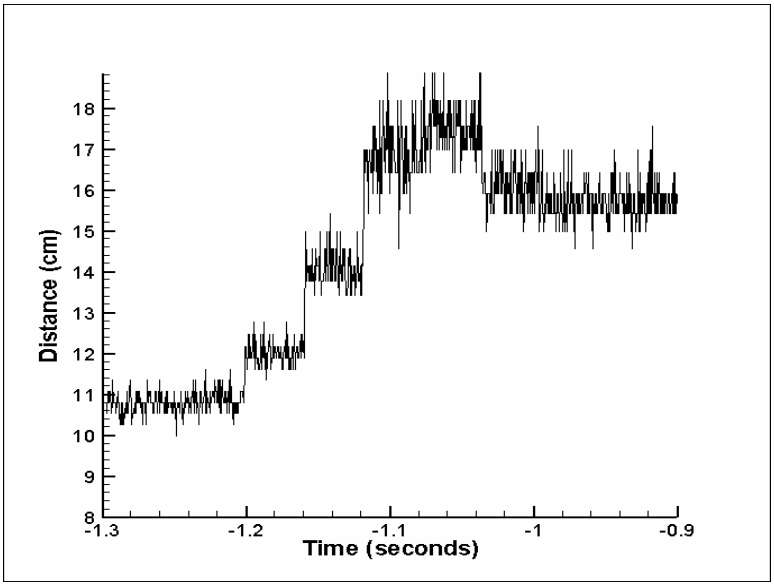

Figure 12.2.2. Time response of energized solenoid C

Figure 12.2.3 shows the response when solenoid C is de-energized. The system takes 400 ms to settle down.

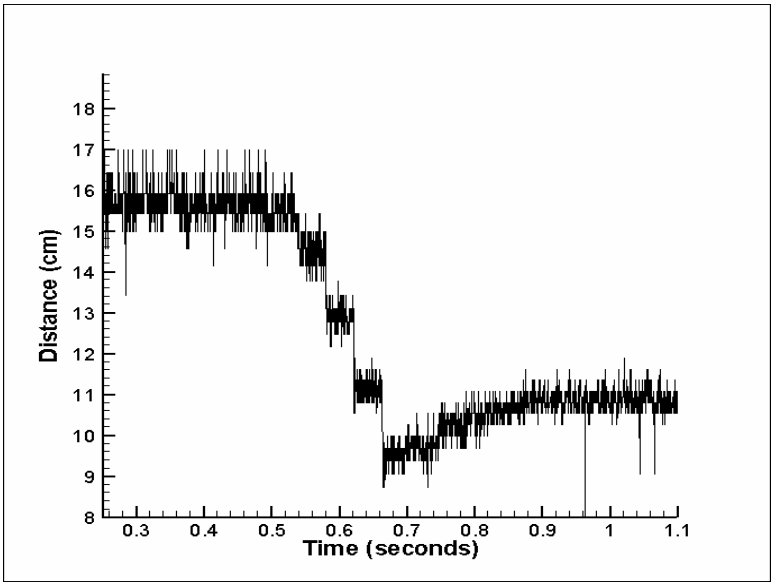

Figure 12.2.3. Time response of de-energized solenoid C

Figure 12.2.4 shows the response when all solenoids all solenoids are enabled simultaneously.

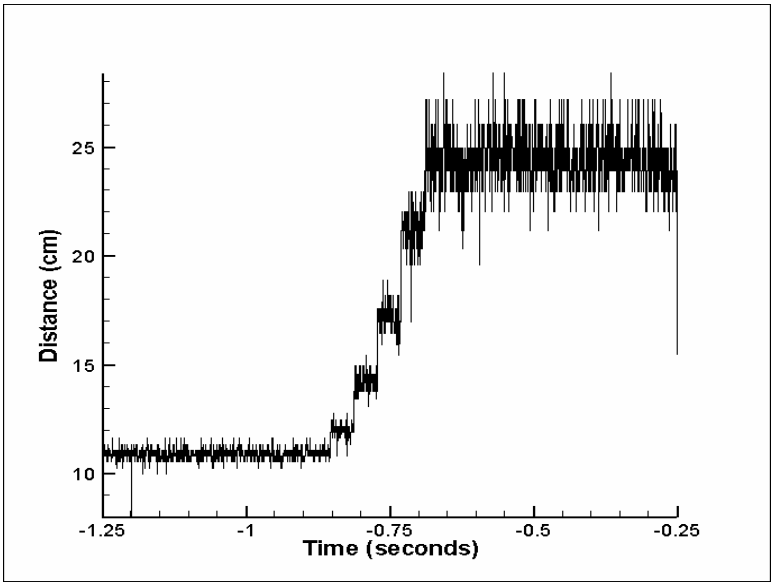

Figure 12.2.4. Time response of all solenoids

From figures 12.2.2, 12.2.3 and 12.2.4, we can see that the time response appears to be in steps. This is due to the timing characteristics of the distance sensor. The distance sensor typically takes 40 ms to make a measurement, hence during that time the output remains

constant. Once a measurement has been made the output changes to the new value and this remains constant until another measurement is completed. Hence the time response curves appear to have steps.

12.3. Dynamic model of solenoid system

The solenoid system is modeled as a three degree of freedom, mass – spring system with frictional damping. Figure 12.3.1 shows the schematic of the dynamic model.

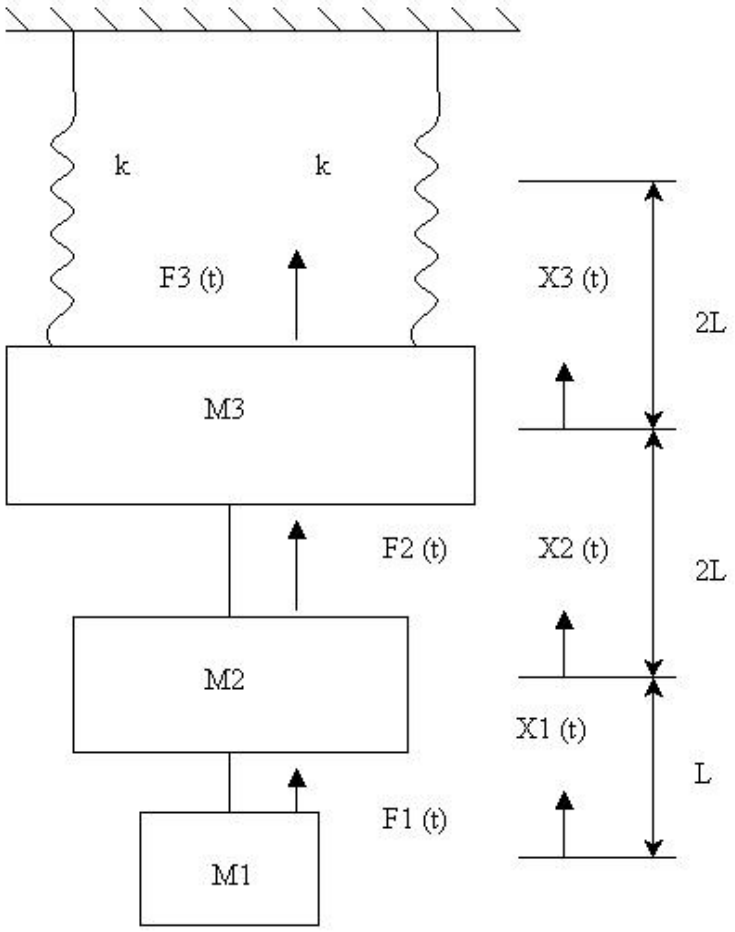

Figure 12.3.1. Dynamic model

The parameter values are as follows:

M1 = 0.2479 Kg

M2 = 1.0185 Kg

M3 = 1.5670 Kg

k = 290.134 N/m

L = 0.0254 m

C = 35 to 55 N.s/m

g = 9.8 m/s^2

The equations of motion are:

$$F1(t) - M1g - c\dot{X}1(t) = M1\ddot{X}1(t)$$

$$F2(t) - (M1 + M2)g - c\dot{X}2(t) = (M1 + M2)\ddot{X}2(t)$$

$$F3(t) - (M1 + M2 + M3)g + 2k(2L - X3(t)) - c\dot{X}3(t) = (M1 + M2 + M3)\ddot{X}3(t)$$

The initial conditions are given by:

X1 (0) = 0 $\quad \dot{X}1(0) = 0$

X2 (0) = L $\quad \dot{X}2(0) = 0$

X3 (0) = 3L $\quad \dot{X}3(0) = 0$

The forces F1, F2 and F3 are the forces exerted by the solenoids. From figures XYZ and ABC, the equations describing the forces in terms of the displacements are as follows:

$$F3(t) = 0.00002X6(t)^4 - 0.0037X6(t)^3 + 0.2436X6(t)^2 - 6.774X6(t) + 94.933$$

$$F2(t) = 0.00002X5(t)^4 - 0.0037X5(t)^3 + 0.2436X5(t)^2 - 6.774X5(t) + 94.933$$

$$F1(t) = 0.0008X4(t)^4 - 0.0477X4(t)^3 + 1.089X4(t)^2 - 11.603X4(t) + 64.381$$

Where X4 (t) = L – X1 (t), X5 (t) = 2L – X2 (t), X6 (t) = 2L – X3 (t), in mm.

These equations are solved numerically using Matlab (appendix 16.10) to predict the behavior of the system. The critical damping constant of the system is about 57 N.s/m. Due to the absence of damping constant data, simulations were performed using four different values for C. Figure 12.3.2 shows the displacement of mass M1 when only solenoid A is activated. The maximum distance moved by the mass in one inch. When the mass reaches a distance of one inch (from its initial position), it impacts mass M2 and instantaneously comes to rest. This is because the mass of M2 is much greater than M1. Also, the impact force exerted by M1 on M2 is negligible to see any significant vibration of the system.

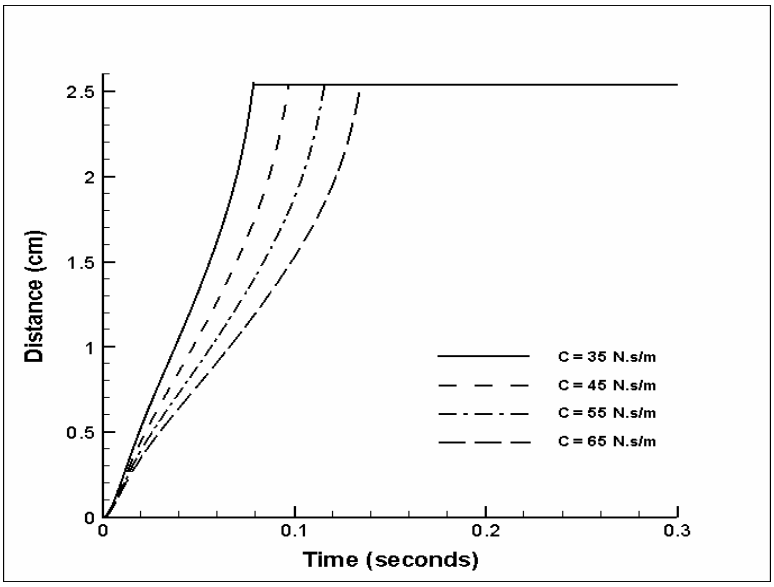

Figure 12.3.2. Predicted response of solenoid A

From figure 12.3.2, we can observe that mass M1 takes about 60 ms - 120 ms to move one inch. From figure 12.2.1, the actual time taken is approximately 100 – 150 ms.

Figure 12.3.3, shows the response of mass M2 when only solenoid 3 is activated. The response shows an overshoot as expected from figure 12.2.2. It can be observed from figure 12.3.3 that as the damping in the system increases, overshoot decreases and settling time increases. The settling time observed from figures 12.2.2 and 12.3.3 is approximately 240 ms.

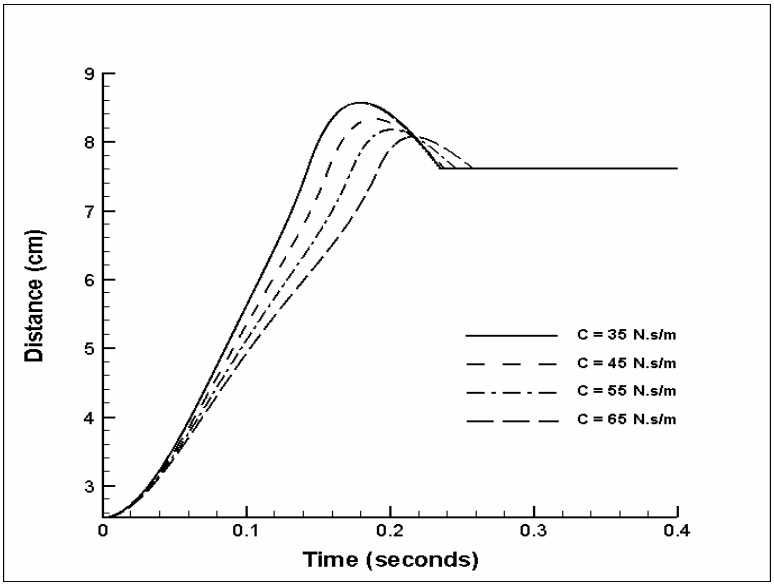

Figure 12.3.3. Predicted response of energized solenoid C

Figure 12.3.4 shows the response of mass M1 when solenoid C is de-energized. The settling time predicted by the model is approximately 375 ms. From figure 12.2.3, the settling time observed is 390 – 400 ms.

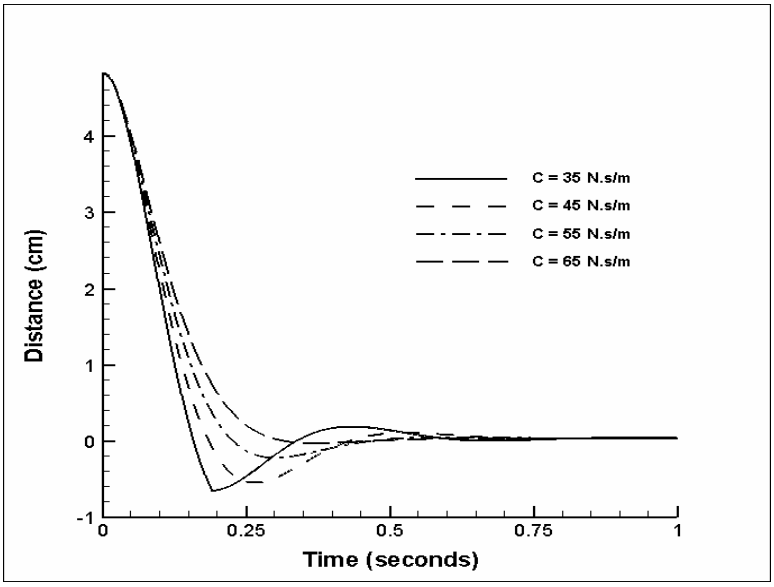

Figure 12.3.4. Predicted response of de-energized solenoid C

Figure 12.3.5 shows the response of mass M1 when all the three solenoids are activated.

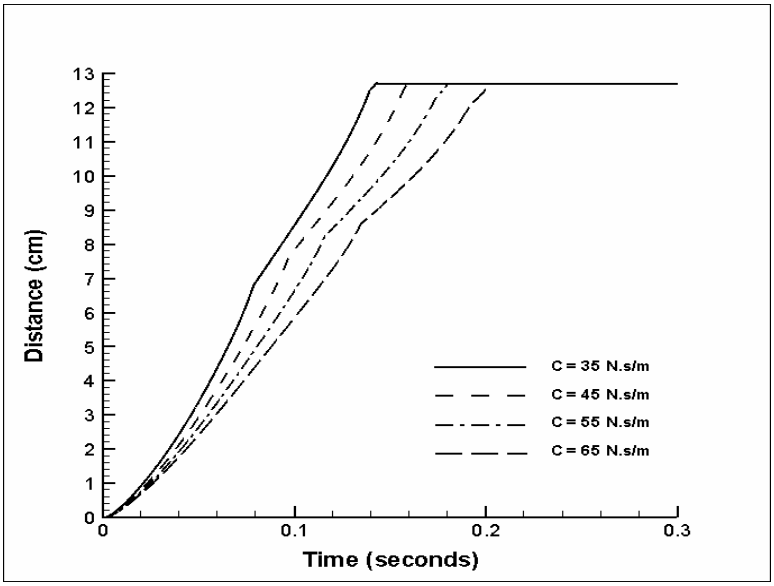

Figure 12.3.5. Predicted response of all solenoids

The model predicts a response time of 160 –180 ms. From figure 12.2.4, the actual response is time 200 – 225 ms.

12.4. Parametric study

From the experimental data and dynamic model, the maximum settling time of the system is approximated to be 400 ms.

Speed of conveyor = 1200 feet per minute
= 20 feet per second

Distance moved by paper sample in 400 ms = 20*0.4 feet
= 8 feet

Processing rate of the sensor system = 60/0.4 samples per minute
= 150 samples per minute

From the above calculations, it is obvious that as long as the distance sensor (for solenoid actuation) is 8 feet ahead of the lignin sensor, the system would perform well at conveyor

speeds of 1200 feet per minute. The processing rate under these conditions would be 150 samples per minute. To increase the processing rate, the settling time of the solenoid system would have to be decreased.

A parametric study was performed to assess the influence of the mass of the system on response time. By comparing the time response curves and the predicted solenoid performance, the damping constant of the system can be approximated to 45 N.s/m. Nondimensionalized mass is defined as the ratio of mass of the model to the mass of the actual system. The actual mass of the system is approximately 2.8334 Kg. This would be equal to unit nondimensionalized mass. Figure 12.4.1 shows the simulation of the response of the system for different nondimensionalized masses.

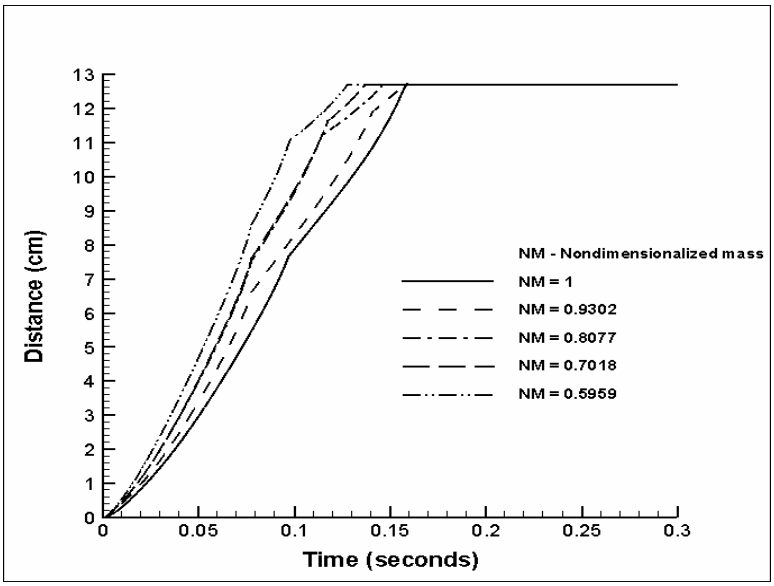

Figure 12.4.1. Effect of nondimensionalized mass

Figure 12.4.2 shows the dependence of response time on nondimensionalized mass. The response time of the actual system is approximately 160 ms. This is equal to unit nondimensionalized time. It is obvious that as the mass of the system decreases, response time also decreases.

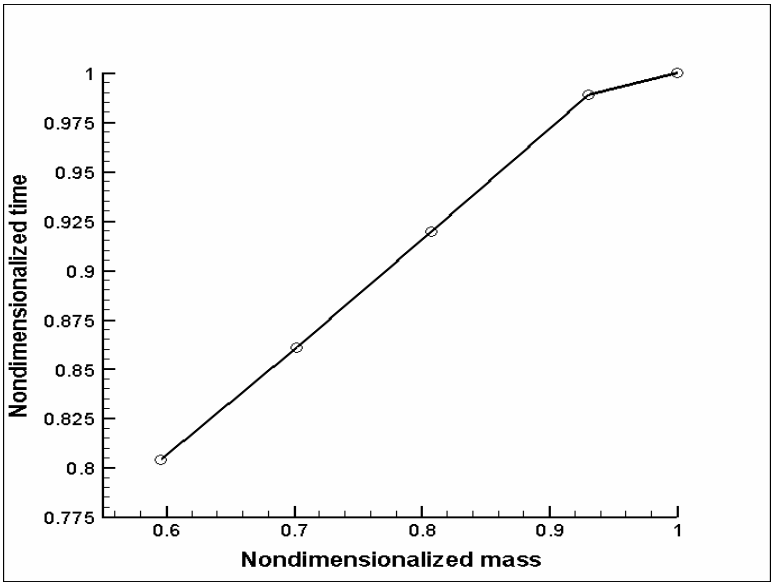

Figure 12.4.2. Response time simulation

The dynamic model developed using Mat lab closely predicts the actual response observed from experimental data. The absence of damping constant data, inaccurate parameter data, and inherent noise in distance sensor output contribute to the error in determining the system characteristics accurately.

13. Micro controller interface

A Motorola MC68HC912B32 micro controller is interfaced to the sensors to do the following

- Read sensor input from lignin and distance sensors
- A/D conversion of input data
- Computation for distance correction
- Logic control of solenoids
- Serial communication with a PC

Figure 13.1 shows the schematic of the micro controller. Figure 13.2 shows the technical layout for the interface circuitry.

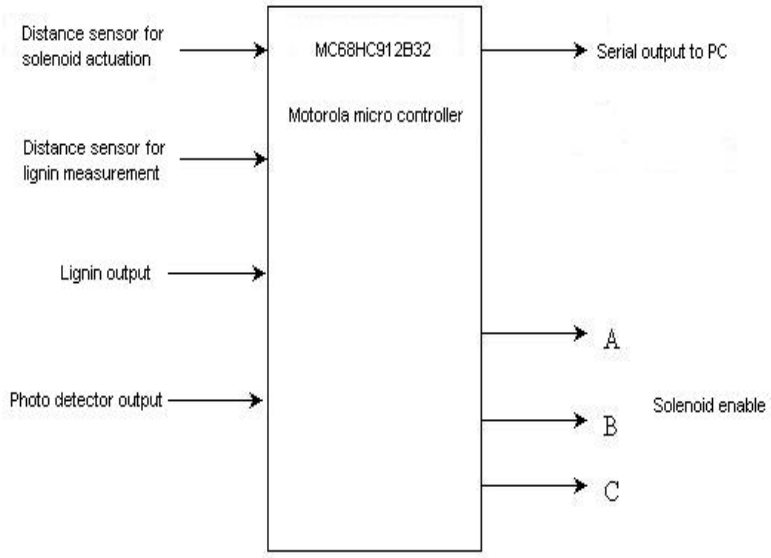

Figure 13.1. Micro controller layout

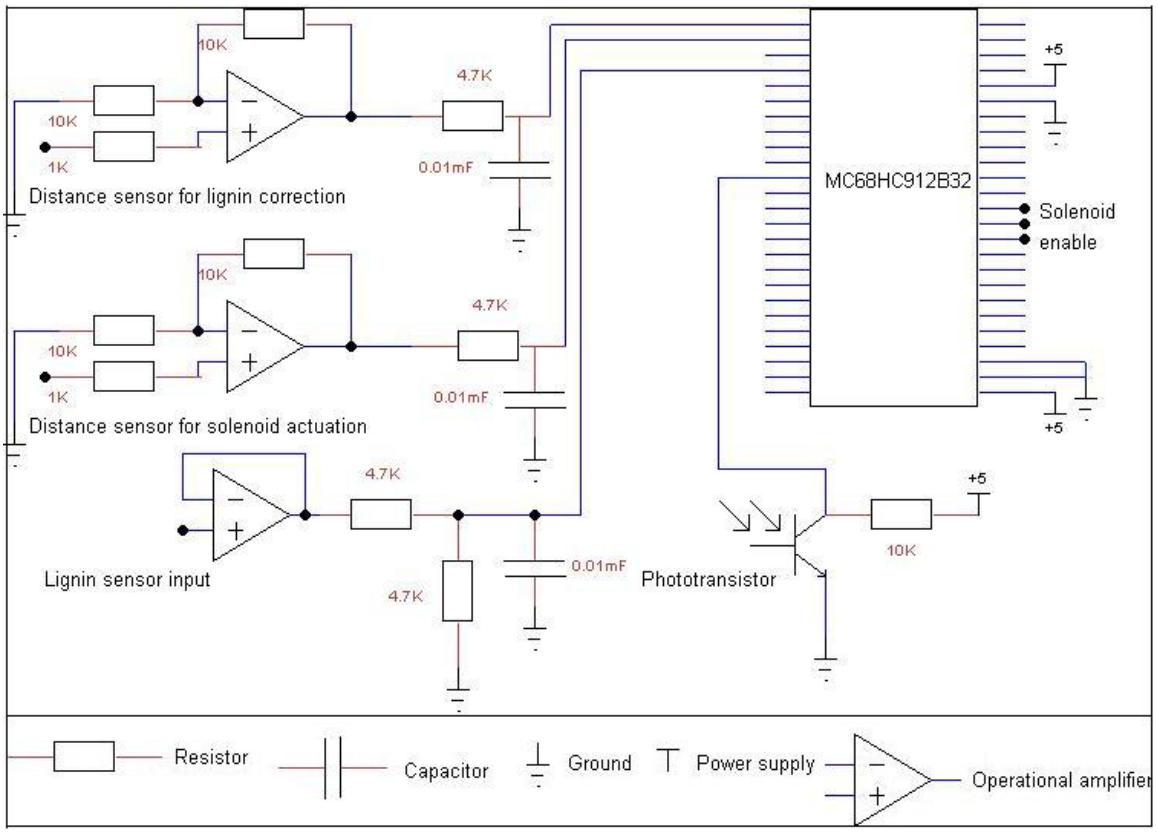

Figure 13.2. Interface circuitry

Distance and lignin sensor signals are amplified using the interface circuitry to give output in the range of 0 – 5 volts. These signals are read into the analog ports on the microprocessor. They are converted into digital values using on board A/D converter. The A/D converter performs 10-bit A/D conversion eight times sequentially on a single channel and stores the results in the ADR registers. Data in the registers is averaged to get the mean digital value.

Lignin response is normalized using the distance correction equation and the corrected lignin output is serially communicated to a PC. Three logic control outputs are used to enable the solenoid driver chips. Figure 13.3 shows the flowchart for the microcontroller.

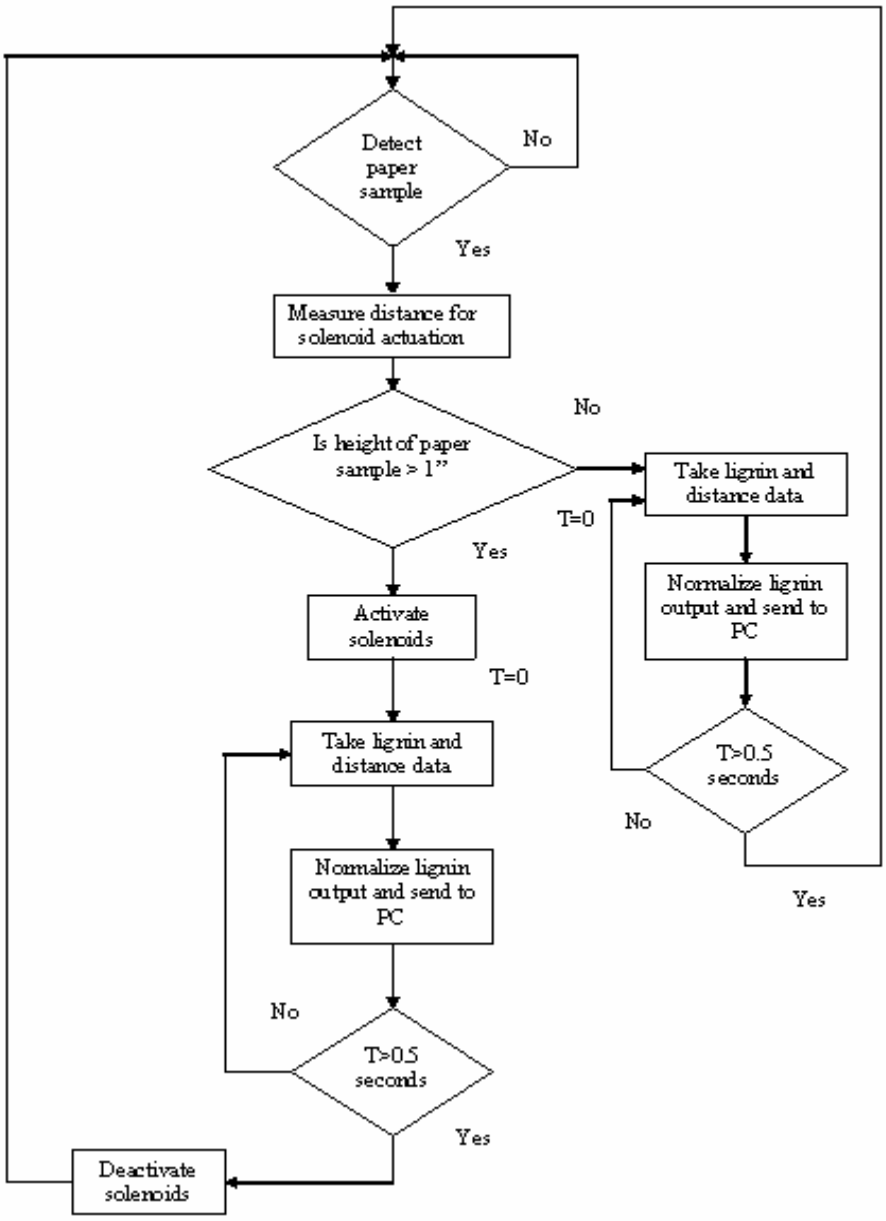

Figure 13.3. Flowchart

14. Conclusion

14.1. Results

A fluorescence sensor to identify paper samples in mixed recycled waste, based on lignin content has been described. The sensor shows excellent correlation with klason lignin content in the pulp. Printed regions in the paper surface and surface color affect the output of the sensor. Using a red laser (635 nm) as an excitation source gives more accurate results when paper samples are presented at varying distances from the sensor head. A cascaded solenoid model is used for moving the sensor head for distance correction. Response time (0.4 seconds) of the solenoid system limits the number of samples sorted per minute. HC12 micro controller interface is provided to the sensor for real time computation and serial communication to a PC. The sensor performed very well at a commercial sorting facility. The sensor is capable of identifying paper samples moving at high speeds and can be successfully used as a part of a multi-sensor system to sort mixed office waste for more efficient recycling. A compact, robust sensor configuration that is simple to implement in the industry has been presented.

14.2. Future work

As mentioned earlier, the critical factor determining the rate of sorting is the response of time of the solenoid system. To increase the throughput of the sorting process, response time has to be decreased. This can be done by experimenting with the cascaded solenoid system or by designing a faster actuating mechanism. As predicted using the dynamic model, response time can be decreased by decreasing the mass of the system.

Accuracy of the sensor output is dependant on the noise in the sensor signals. Lignin sensor has a good signal to noise ratio, whereas the distance sensors introduce significant noise into the system. This is can be eliminated by using good filter circuits.

The sensor has to be tested at a commercial sorting facility to assess its performance under shop floor conditions. Then it can be integrated into a multi sensor system for paper sorting.

15. References

1. Ammineni, C., Design of lignin sensor for identification of waste paper grades for an automatic waste paper sorting system, in Mechanical and Aerospace Engineering department. 2001, North Carolina State University, Raleigh, NC, USA.
2. Olmstead, J. A. and Gray, D. G., "Fluorescence spectroscopy of cellulose, lignin and mechanical pulps: A review", Journal of Pulp and Paper science 23(12), 1997.
3. Bergstrom, H., et al, Identification of different substances in paper using fluorescence spectroscopy, Proc. International printing graphic arts conference, Halifax, NS, 1994.
4. Nilsson, M., Malmqvist, L., Carlsson, J., Red fluorescence sensor for non-contact on line measurements in paper production, Optical engineering, 2001. 40(8): Pages 1674 – 1681.
5. Saariaho, A., et al, Ultra violet resonance Raman spectroscopy in lignin analysis: Determination of characteristic vibrations of p-hydroxyphenyl, guaiacyl, and syringyl lignin Structures, Applied Spectroscopy, 2003. 57(1): Pages 58-66.
6. Argyropoulous, D. and S. Menachem., Chapter 12: Lignin, in Biopolymers from renewable resources, D. Kaplan, Editor. 1998, Springer Verlag: New York. Pages 292-322.
7. Smook, G., Handbook for Pulp and Paper Technologists. 2nd edition ed. 1992, Bellingham, WA: Angus Wilde Publications.
8. Olmstead, J. and D. Gray., Fluorescence Spectroscopy of Cellulose, Lignin, and Mechanical Pulps - A review. Journal of Pulp and Paper Science, 1997. 23(12).
9. Toner, S. and K. Plitt., Spectrophotofluorimetric Studies of Degraded Cotton Cellulose. Tappi Journal, 1962. 45(8): Page 681.
10. Castellan, A. and R. Davidson., Steady-state and dynamic fluorescence emission from Abies wood", J Photochemistry and Photobiology, 1994. 78(3): Pages 275-279.

11. Billa, E., E. Koutsoula, and E.G. Koukios., Fluorescence Analysis of Pulps. Journal of Bioresource Technology, 1999. 67: Pages 25-33.
12. Eduardo, A., et al., The use of fluorescent probes in the characterization of lignin: The distribution, by energy, of fluorophores in Eucalyptus grandis lignin", Journal of Photochemistry and Photobiology, 2001. 138: Pages 253-259.
13. Bublitz, W. and T. Meng., Applying Waste Liquor Fluorescence to control Pulp Quality. Svensk Papperstidn, 1979.
14. Bublitz, W. and D. Wenzel., Laser-Induced Fluorescence of Lignins with Excitation from 457 to 621 Nanometers. Journal of Wood Chemical Technology, 1991. 11(1): Pages 105-115.
15. Berthold., Fluorescence analyzer for lignin. 1993: USA.
16. Jeffers, On-line measurement of lignin in wood pulp by color shift of fluorescence. 1996.
17. Lundquist, K., B. Josefsson, and G. Nyquist., Analysis of Lignin Products by Fluorescence Spectroscopy. Holzforschung, 1978.
18. Carlsson, J., et al. Application of Optical Fluorescence Spectroscopy to Paper Production, International Paper Physics Conference. 1999.
19. Ramasubramanian, M., R. Venditti, and C. Ammineni., Optical sensor for non-contact measurement of lignin content in high speed moving paper surfaces. IEEE Sensors Journal (in review), 2003.

16. Appendices

16.1. Technical specifications for photon counting module (MD962)

Supply voltage	5 V dc
Supply current	< 280 mA
Settling time	< 1s (time to stabilize HV after supply voltage applied)
Over-illumination protection: active quenching control (internal)	
Current to voltage conversion factor 1 V/ 20nA (other values on request)	
Output signal	0 ... 10 V dc
Output offset	± 3mV
Gain	up to 1 x 108, via internal potentiometer (or by external control voltage 0...3 V via external opamp circuit)
Active Quenching Control	TTL-Pulse, active high
RESET	internal via timer, typical 1 second, external via 5 V-pulse
Frequency bandwidth	DC to 1 kHz (other values on request, max. 20 kHz)
GATE voltage Vgate	5 V: h to l set time Vca to Vch-ent +100 V: ~ 150 µs 5 V: l to h set time Vca to Vch-ent - 100 V: ~ 150 µs
High voltage pre-adjusted	1500 volts

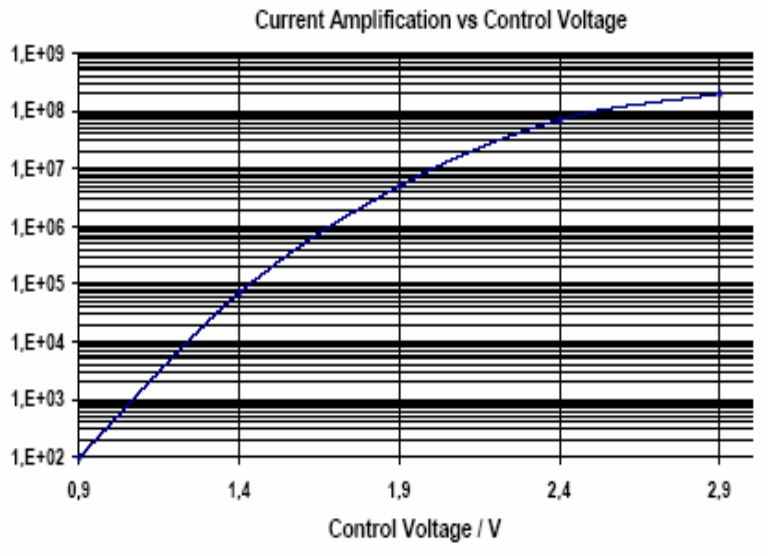

Figure 16.1.1. Gain characteristic of photon counting module

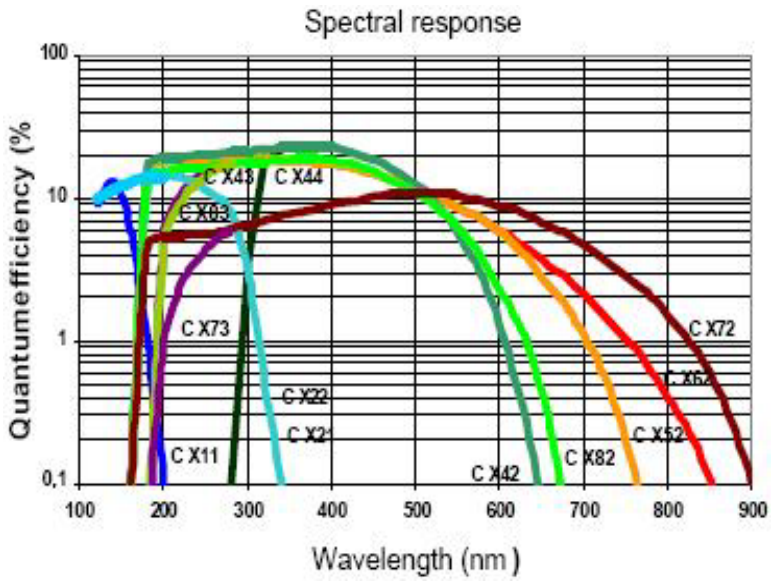

Figure 16.1.2. Quantum efficiency of photon counting module

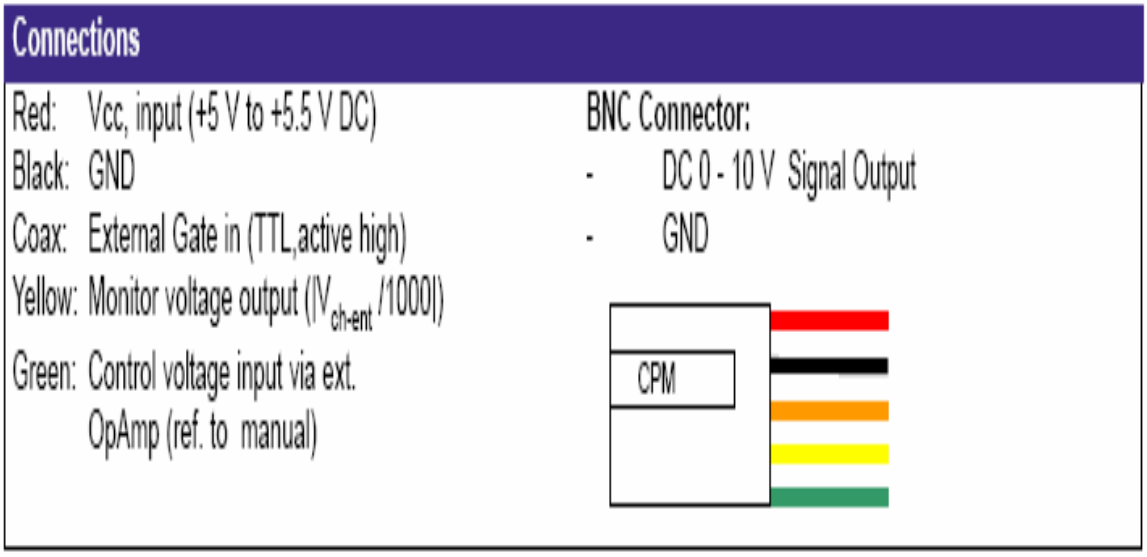

Figure 16.1.3. Wiring diagram for photon counting module

16.2. Technical specifications for green laser (VLM-532-43LCC)

Dimension	54 mm X 13 mm
Weight	36 g
Construction	Brass

Operating voltage	2.7 – 3.3 volts
Operating current	270 – 350 mA
Wavelength	532 nm
Output power	15 mW
Spot size	< 6 mm @ 5 meters, < 18 mm @ 30 meters
Half divergence angle	<0.3 mRad
Operating temperature	20 – 30 centigrade
Output power stability	< 10% @ 25 centigrade after 10 minutes warm up
Life time	> 4000 hours

16.3. Technical specifications for red laser (VM63514)

Wavelength	635 nm
Polarization	Linear 100:1
Max ambient temperature	40 centigrade
Operating voltage	2.8 – 3.5 volts
Operating current	85 mA
Beam divergence	< 1.3 mRad
Output power	15 mW

16.4. Filter specifications

Table 16.4.1. 03FIV358 specifications

Shape	Round
Diameter:	12.5 mm
Center Wavelength	700 +10/-0 nm
Peak Transmission	45%
FWHM	40 ± 8 nm

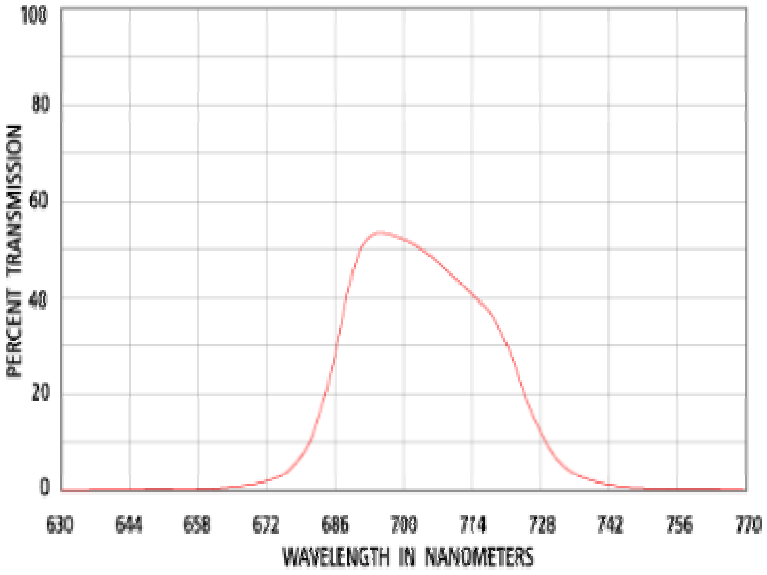

Figure 16.4.1. 03FIV358 transmission spectrum

Table 16.4.2. 03FIL252 specifications

Shape	Round
Diameter:	12.5 mm
Center Wavelength	650 +3/-0 nm
Peak Transmission	45%
FWHM	10 ± 2 nm

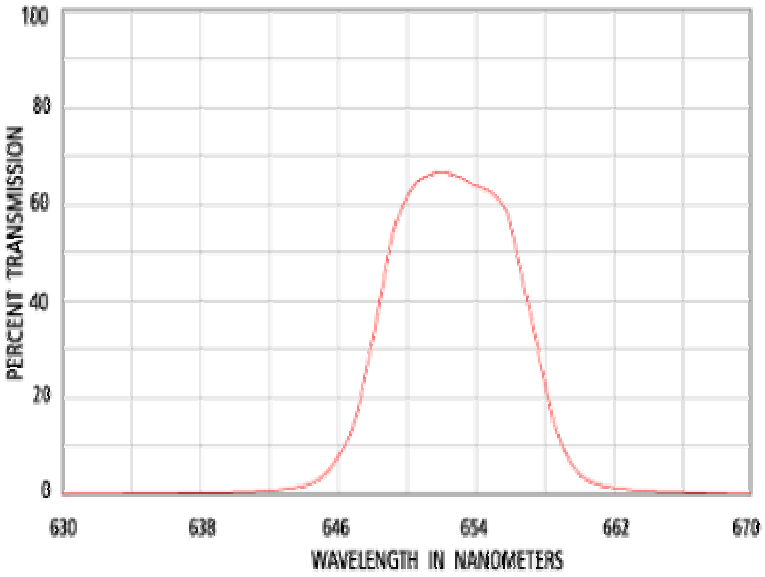

Figure 16.4.2. 03FIL252 transmission spectrum

Table 16.4.3. 03FIL251 specifications

Shape	Round
Diameter:	12.5 mm
Center Wavelength	690 +3/-0 nm
Peak Transmission	50%
FWHM	10 ± 2 nm

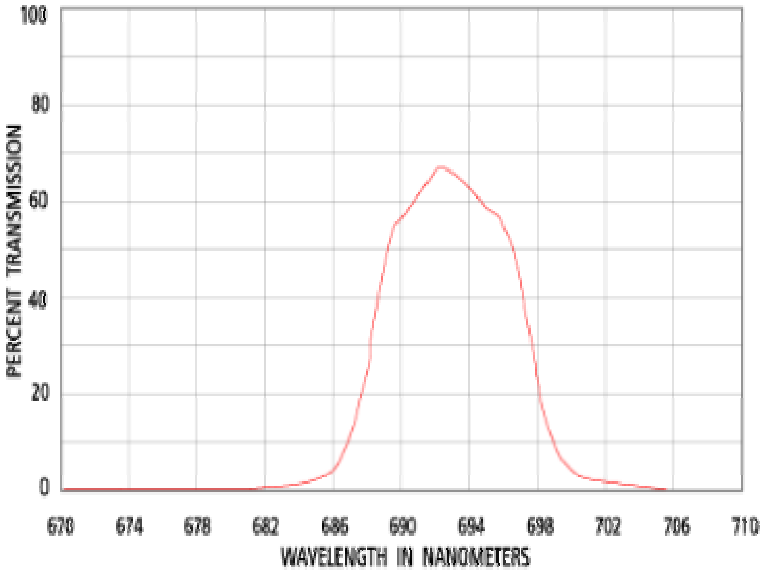

Figure 16.4.3. 03FIL251 transmission spectrum

Table 16.4.4. 03FIB314 specifications

Shape	Round
Diameter:	12.5 mm
Center Wavelength	650 +25/-0 nm
Peak Transmission	70%
FWHM	80±16 nm

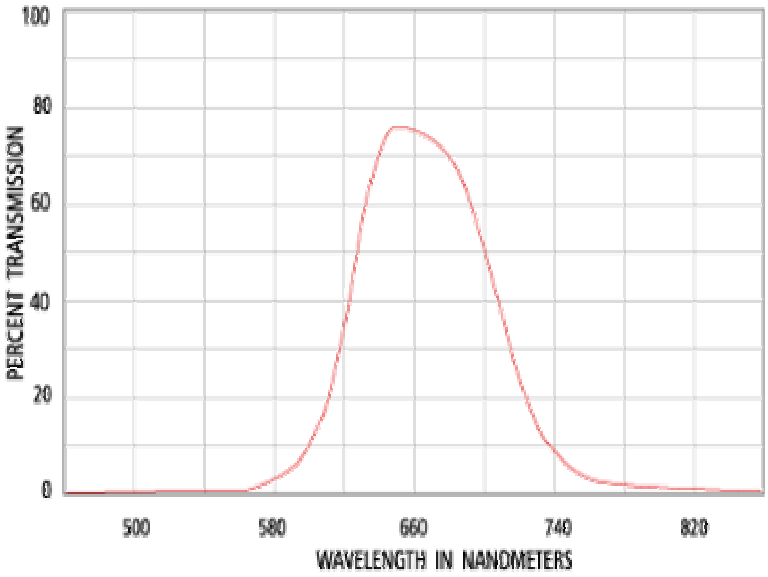

Figure 16.4.4. 03FIB314 transmission spectrum

16.5. Color samples

Figure 16.5.1. Color 11A

Figure 16.5.2. Color 11B

Figure 16.5.3. Color 11C

Figure 16.5.4. Color 11D

Figure 16.5.5. Color 12A

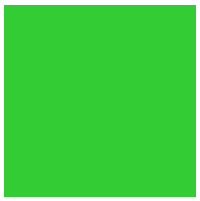

Figure 16.5.6. Color 12B

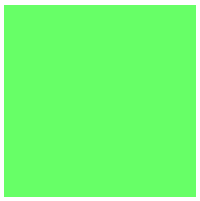

Figure 16.5.7. Color 12C

Figure 16.5.8. Color 12D

Figure 16.5.9. Color 13A

Figure 16.5.10. Color 13B

Figure 16.5.11. Color 13C

Figure 16.5.12. Color 13D

Figure 16.5.13. Color 14A

Figure 16.5.14. Color 14B

Figure 16.5.16. Color 14C

Figure 16.5.16. Color 14D

Figure 16.5.17. Color 15A

Figure 16.5.18. Color 15B

Figure 16.5.19. Color 15C

Figure 16.5.20. Color 15D

Figure 16.5.21. Color 16A

Figure 16.5.22. Color 16B

Figure 16.5.23. Color 16C

Figure 16.5.24. Color 16D

Figure 16.5.25. Color 17A

Figure 16.5.26. Color 17B

Figure 16.5.27. Color 17C

Figure 16.5.28. Color 17D

Figure 16.5.29. Color 18A

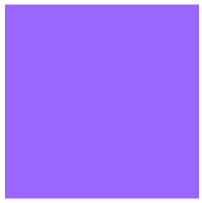

Figure 16.5.30. Color 18B

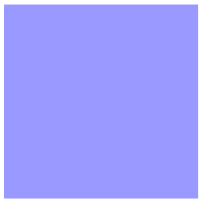

Figure 16.5.31. Color 18C

Figure 16.5.32. Color 19A

Figure 16.5.33. Color 19B

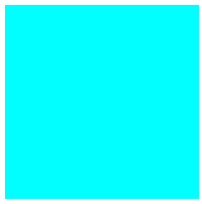

Figure 16.5.34. Color 19C

Figure 16.5.35. Color 20A

Figure 16.5.36. Color 20B

Figure 16.5.37. Color 20C

16.6. Photodiode specifications

The following figure shows the spectral response of the photodiode (C2386-45K).

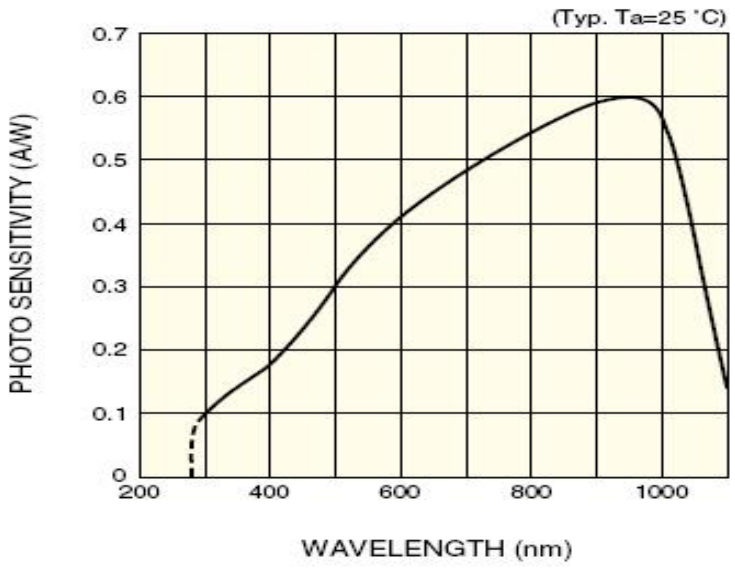

Figure 16.6.1. Spectral response of photodiode

16.7. Distance sensor data

The following figures and tables show the opto - electrical and distance characteristics for the distance sensors (GP2D120 and GP2D12).

Table 16.7.1 Opto - electrical characteristics for GP2D12 and GP2D120

Parameter	Symbol	Conditions	Min.	Typ.	Max.	Unit
Measuring distance range	ΔL	(*1)	4	-	30	cm
Output terminal voltage	Vo	L=30cm (*1)	0.25	0.4	0.55	V
Output voltage difference	ΔVo	Output change at L change (30cm → 4cm) (*1)	1.95	2.25	2.55	V
Average supply current	Icc	L=30cm (*1)	-	33	50	mA

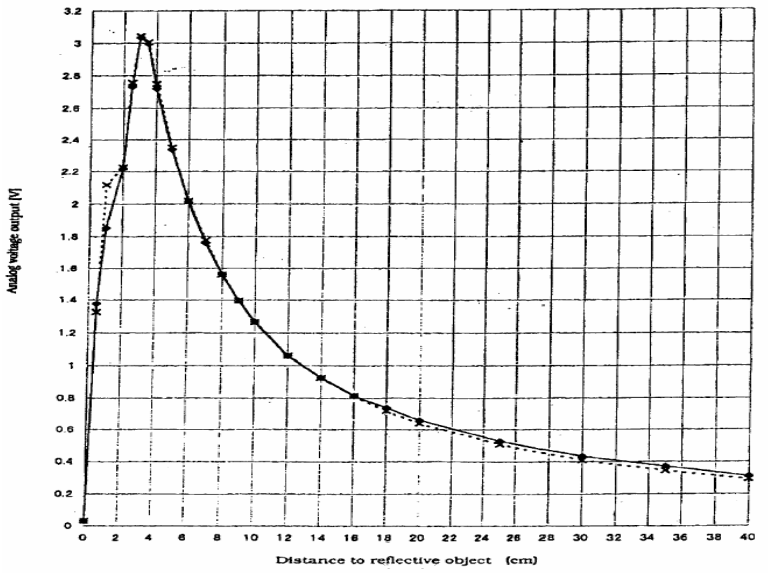

Figure 16.7.1. Distance characteristic curve for GP2D120

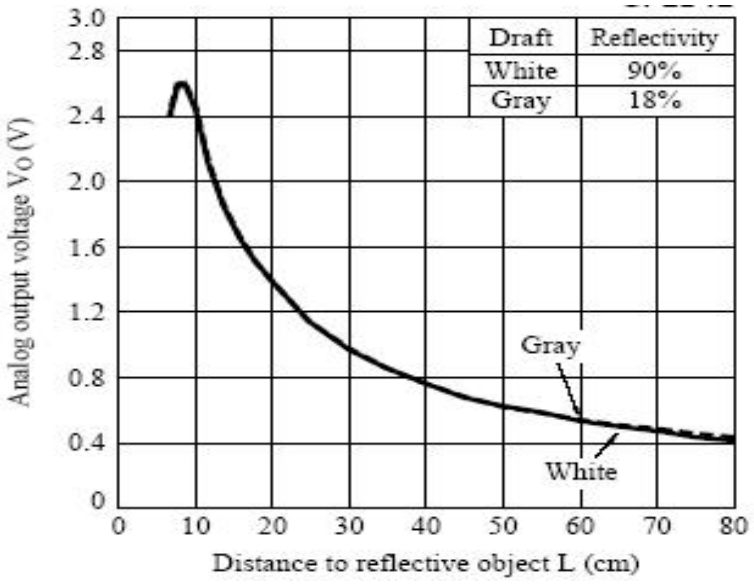

Figure 16.7.2. Distance characteristic curve for GP2D12

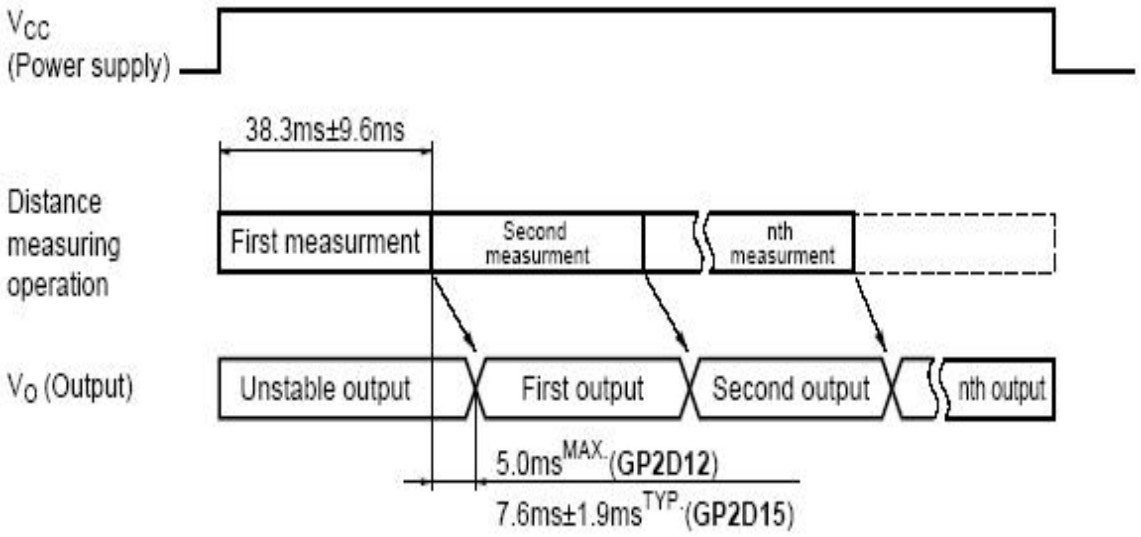

Figure 16.7.3. Timing chart for GP2D120 and GP2D12

16.8. Solenoid data

Specifications for solenoid A (C34-273-M-33) and solenoid B (194580-25) are given in the following figures and tables.

Table 16.8.1. Solenoid A specifications

Continuous Duty Cycle	At 20°C ambient temperature
Intermittent Duty Cycle	See below
Holding Force	6.8 lbs (30.2 N) at 20°C
Coil Insulation	Class "A": 105°C max. temperature standard. Other temperature classes are available
Coil Termination	1/4" QC
Plunger Weight	1.2 oz. (34.9 g)
Total Weight	6.8 oz. (192.8 g)
Dimensions	See page G41

Table 16.8.2. Solenoid A performance characteristics

Maximum Duty Cycle	100%	50%	25%	10%
Maximum ON Time (sec) when pulsed continuously	∞	45	20	7
Maximum ON Time (sec) for single pulse	∞	453	160	47
Watts (@ 20°C)	10	20	40	100
Ampere Turns (@ 20°C)	1188	1684	2377	3763

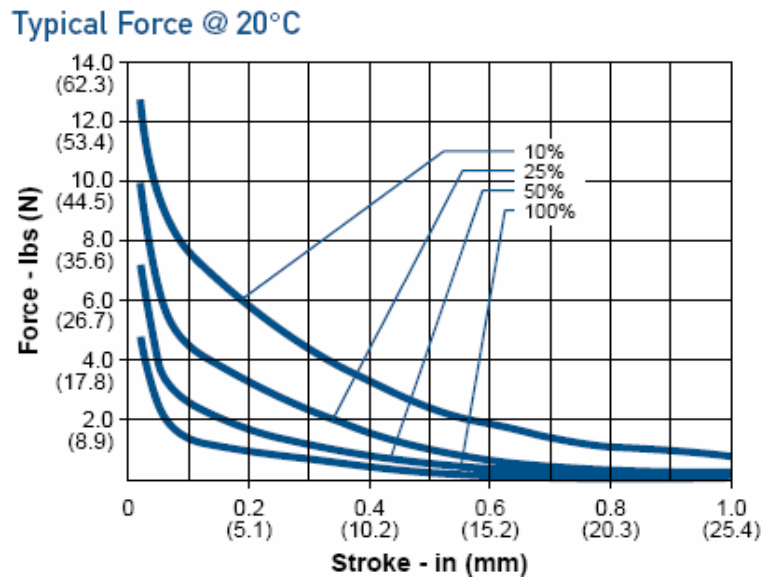

Figure 16.8.1. Solenoid A force curves

Table 16.8.3. Solenoid B specifications

Dielectric Strength	1000 VRMS
Recommended Minimum Heat Sink	Maximum watts dissipated by solenoid are based on an unrestricted flow of air at 20°C, with solenoid mounted on the equivalent of an aluminum plate measuring 10" square by ⅛" thick
Coil Resistance	±5% tolerance
Holding Force	18 lbs (80.06 N) @ 20°C
Weight	2.25 lb (1.02 kg)
Dimensions	Ø1.75" x 4.71" L (See page E24)

Table 16.8.4. Solenoid B performance characteristics

Maximum Duty Cycle	100%	50%	25%	10%
Maximum ON Time (sec) when pulsed continuously[1]	∞	882	209	54
Maximum ON Time (sec) for single pulse[2]	∞	1,200	528	162
Watts (@ 20°C)	20	40	80	200
Ampere Turns (@ 20°C)	2923	4133	5844	9238

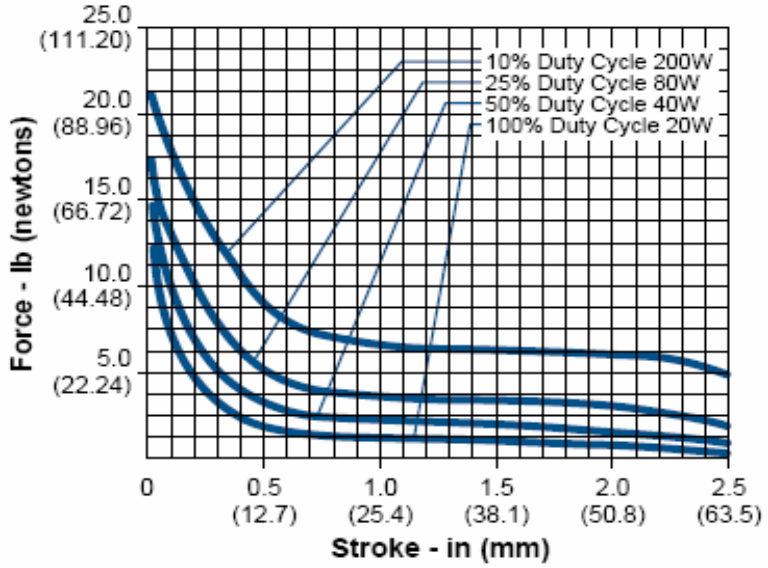

Figure 16.8.2. Solenoid B force curves

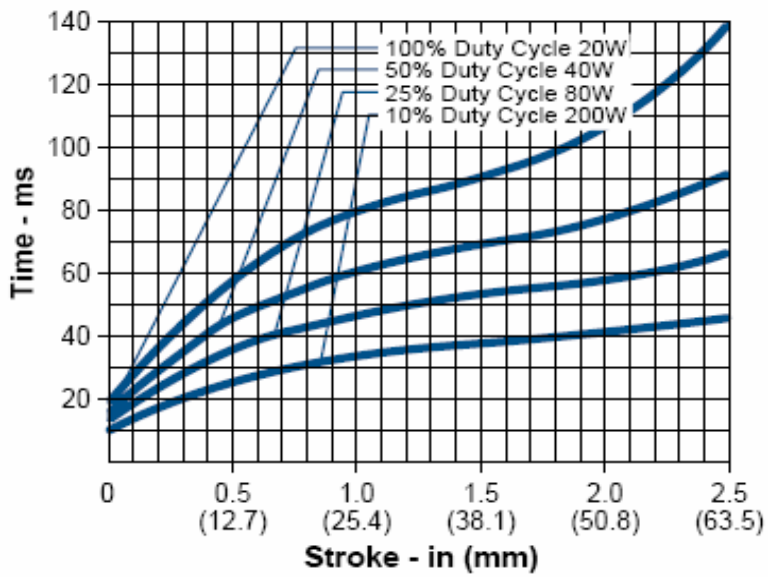

Figure 16.8.3. Solenoid B response time curves

16.9. HC12 code

```
#include <912b32.h>
#include <STDIO.h>
#include <pvectors.c>
#include <math.h>
#define inch 2.54
#define Dmax 27

#define ADR0 (* (volatile unsigned int *) 0x70)
#define ADR1 (* (volatile unsigned int *) 0x72)
#define ADR2 (* (volatile unsigned int *) 0x74)
#define ADR3 (* (volatile unsigned int *) 0x76)
#define ADR4 (* (volatile unsigned int *) 0x78)
#define ADR5 (* (volatile unsigned int *) 0x7a)
#define ADR6 (* (volatile unsigned int *) 0x7c)
#define ADR7 (* (volatile unsigned int *) 0x7e)
```

```
//Vmax is the maximum voltage of the distance sensor when the surface is at
//a distance of 3.3 cm from the sensor. The distance vs. voltage curve is
//normalized using this value
//inch is a constant for 1 inch = 2.54 cm
//Dmax is the height at which the distance sensor is place from the conveyor or
//surface. For testing it is 20 cm


extern int _textmode;   //These lines map the '\n' character of printf to
_textmode = 1;          //the character pair carriage return and linefeed
                        //So output appears as expected on a windows terminal

void delay100microsec(void);
float analog(int c);
void print(float n);
float normalizedlignin(float L, float D);

float Dcal,u,v,w;
float Hs,Hssum,Hstemp[10],Vsi,Hsi;
float Hl,Hlsum,Hltemp[10],Vli,Hli;
float Li,Ln;
int i,j,k;
double x,y,z;

void main(void)
        {
                setbaud(BAUD9600); //set baud rate to 9600
                TSCR=0x80;         //Enable timer
                TMSK2=0x02;        //Set timer freq = Eclk/4 = 2MHz
                ATDCTL2=0x80;      //Enable A to D converter
```

```
delay100microsec(); //Wait for 100 micro sec to let ATD stabilize
ATDCTL4=0x81;       //Final sample time = 2 ATD clock
                    //Prescaler = div by 4
DDRDLC=0x0F;        //PDLC0 - lignin binary output PDLCi - solenoid i
                    //enable (i=1,2,3)
PORTDLC=0;          //Disable solenoid outputs
PWEN=0;             //PORTP4 lignin distance sensor enable input
DDRP=0xBF;          //PORTP7 is input rest are output
PORTP=0;            //Set all PORTP output pins to 0

Dcal=25.4;
u=0.1667;
v=0.03714;
w=-0.002245;
x=-1.073*pow(10,-3.0);
y=1.713*pow(10,-5.0);
z=9.466*pow(10,-6.0);

while (1)
{
if(PORTP==0x40)     //Read distance sensor data when photo detector
                    //goes high i.e., paper sample is detected
{
Hssum=0;
for(i=0;i<10;i++)
{
Vsi=analog(2)/204.6;
Hsi=(-0.7607*pow(Vsi,3))+(9.6992*pow(Vsi,2))-(44.532*Vsi)+(83.526);
Hstemp[i]=Hsi;
Hssum=Hssum+Hstemp[i];
}
```

```
Hs=((Dmax)-(Hssum/10.0));
if (Hs<0)        //If there is an error in height measurement print error
printf("\nError");
if ((Hs>0)&&(Hs<=2.54))     //Take distance and lignin measurements
                            //and correct for height of paper sample.
{                           //Send output to PC via serial port
for(j=0;j<500;j++)
{
Hlsum=0;
for(k=0;k<10;k++)
{
Vli=analog(0)/204.6;
Hli=(-0.3586*pow (Vli,3))+(4.3038*pow(Vli,2))-(18.556*Vli)+(29.439);
if(Hli<0)
Hli=0;
Hltemp[k]=Hli*10;
Hlsum=Hlsum+Hltemp[k];
}
Hl=Hlsum/10.0;
Li=analog(3)/1023.0;
Ln=normalizedlignin(Li,Hl);
if(Ln<0)
Ln=0;
if(Ln>1)
Ln=1;
printf("\n");
print(Ln);
}
}
if ((Hs>2.54)&&(Hs<=5.08))
{
```

```
PORTDLC=0x08; //Fire solenoid 3
for(j=0;j<500;j++)
{
Hlsum=0;
for(k=0;k<10;k++)
{
Vli=analog(0)/204.6;
Hli=(-0.3586*pow(Vli,3))+(4.3038*pow(Vli,2))-(18.556*Vli)+(29.439);
if(Hli<0)
Hli=0;
Hltemp[k]=Hli*10;
Hlsum=Hlsum+Hltemp[k];
}
Hl=Hlsum/10.0;
Li=analog(3)/1023.0;
Ln=normalizedlignin(Li,Hl);
if(Ln<0)
Ln=0;
if(Ln>1)
Ln=1;
printf("\n");
print(Ln);
}
PORTDLC=0;
}
if((Hs>5.08)&&(Hs<=7.62))
{
PORTDLC=0x04; //Fire solenoid 2
for(j=0;j<500;j++)
{
Hlsum=0;
```

```
for(k=0;k<10;k++)
{
Vli=analog(0)/204.6;
Hli=(-0.3586*pow(Vli,3))+(4.3038*pow(Vli,2))-(18.556*Vli)+(29.439);
if(Hli<0)
Hli=0;
Hltemp[k]=Hli*10;
Hlsum=Hlsum+Hltemp[k];
}
Hl=Hlsum/10.0;
Li=analog(3)/1023.0;
Ln=normalizedlignin(Li,Hl);
if(Ln<0)
Ln=0;
if(Ln>1)
Ln=1;
printf("\n");
print(Ln);
}
PORTDLC=0;
}
if ((Hs>7.62)&&(Hs<=10.16))
{
PORTDLC=0x0C; //Fire solenoids 2,3
for(j=0;j<500;j++)
{
Hlsum=0;
for(k=0;k<10;k++)
{
Vli=analog(0)/204.6;
Hli=(-0.3586*pow(Vli,3))+(4.3038*pow(Vli,2))-(18.556*Vli)+(29.439);
```

```
if(Hli<0)
Hli=0;
Hltemp[k]=Hli*10;
Hlsum=Hlsum+Hltemp[k];
}
Hl=Hlsum/10.0;
Li=analog(3)/1023.0;
Ln=normalizedlignin(Li,Hl);
if(Ln<0)
Ln=0;
if(Ln>1)
Ln=1;
printf("\n");
print(Ln);
}
PORTDLC=0;
}
if((Hs>10.16)&&(Hs<=12.7))
{
PORTDLC=0x06; //Fire solenoids 1,2
for(j=0;j<500;j++)
{
Hlsum=0;
for(k=0;k<10;k++)
{
Vli=analog(0)/204.6;
Hli=(-0.3586*pow(Vli,3))+(4.3038*pow(Vli,2))-(18.556*Vli)+(29.439);
if(Hli<0)
Hli=0;
Hltemp[k]=Hli*10;
Hlsum=Hlsum+Hltemp[k];
```

```
}
Hl=Hlsum/10.0;
Li=analog(3)/1023.0;
Ln=normalizedlignin(Li,Hl);
if(Ln<0)
Ln=0;
if(Ln>1)
Ln=1;
printf("\n");
print(Ln);
}
PORTDLC=0;
}
if((Hs>12.7) && (Hs<=15.24))
{
PORTDLC=0x0E; //Fire solenoids 1,2,3
for(j=0;j<500;j++)
{
Hlsum=0;
for(k=0;k<10;k++)
{
Vli=analog(0)/204.6;
Hli=(-0.3586*pow(Vli,3))+(4.3038*pow(Vli,2))-(18.556*Vli)+(29.439);
if(Hli<0)
Hli=0;
Hltemp[k]=Hli*10;
Hlsum=Hlsum+Hltemp[k];
}
Hl=Hlsum/10.0;
Li=analog(3)/1023.0;
Ln=normalizedlignin(Li,Hl);
```

```
                if(Ln<0)
                Ln=0;
                if(Ln>1)
                Ln=1;
                printf("\n");
                print(Ln);
                }
                PORTDLC=0;
                }
                if(Hs>15.24)
                {
                printf("\nSample too close to sensor");
                }
                }
                }
        }
float normalizedlignin (float L, float D)
        {
                        //Function to adjust for height variation of paper
                        // samples which are 1 to 2 inches from the distance
                        //sensor using green laser
                        //Surface plot G25
                        float Lconn,Lcond,Lcon,Lcal1,Lcal2,Lcal;

                        Lconn=(L-u-(w*D)-(y*pow(D,2.0)));
                        Lcond=(v+(x*D)+(z*pow(D,2.0)));
                        Lcon=Lconn/Lcond;
                        Lcal1=(u+(v*Lcon)+(w*Dcal)+(x*Dcal*Lcon));
                        Lcal2=((y*pow(Dcal,2))+(z*Lcon*pow(Dcal,2)));
                        Lcal=Lcal1+Lcal2;
                        return Lcal;
```

```
        }

float analog(int c)
        {
                float result;                   //Select single scan single channel
                ATDCTL5=64+c;                   //Select 8 conversions and channel number
                while (!(ATDSTAT & 0x8000)); //Wait for conversion complete flag
                result=((ADR0>>6)+(ADR1>>6)+(ADR2>>6)+(ADR3>>6)+
                (ADR4>>6)+(ADR5>>6)+(ADR6>>6)+(ADR7>>6))/8.0;
                return result;
        }
void delay100microsec(void)          //Function to get a delay of 100 microseconds
         {
          unsigned int delay_var;
          delay_var=TCNT+200;
          while(delay_var>TCNT);
         }
void print(float n)                  //Function to print a floating point number
        {
                int j,i[3];
                float f[4];

                f[0]=n;
                for(j=0;j<=2;j++)
                    {
                        i[j]=f[j];
                        f[j+1]=(f[j]-i[j])*10;
                    }
                printf("%d.%d%d",i[0],i[1],i[2]);
        }
```

16.10. Matlab code

```
L = 0.0254; %1 inch in metric
k = 290.134; %Spring constant in N/m
m1 = 0.2479;  %kg
m2 = 1.0185;
m3 = 1.5670;
g = 9.8;          %m/s^2
c = 55;

a1 = 0.0008;
b1 = -0.0477;
c1 = 1.089;
d1 = -11.603;
e1 = 61.381;

a2 = 2*10^(-5);
b2 = -0.0037;
c2 = 0.2436;
d2 = -6.774;
e2 = 94.933;

a3 = 2*10^(-5);
b3 = -0.0037;
c3 = 0.2436;
d3 = -6.774;
e3 = 94.933;

y1(1) = 0;
y2(1) = 0;
y3(1) = L;
y4(1) = 0;
y5(1) = 3*L;
y6(1) = 0;

t = 0:0.0001:0.5;
h = 0.0001;

for i = 2:5001

if(y1(i-1)<L)
   k1a = h*y2(i-1);
   y1(i) = y1(i-1) + k1a;
   ya(i) = (L- y1(i))*10^(3);
   F1(i) = ((a1*(ya(i)^4)) + (b1*(ya(i)^3)) + (c1*(ya(i)^2)) + (d1*ya(i)) + e1)-(c*y2(i-1));
```

```
   k2a = h*((F1(i)/m1) - g);
   y2(i) = y2(i-1) + k2a;
else
   y1(i) = L;
   y2(i) = 0;
end

if(y3(i-1)<(3*L))
   k1b = h*y4(i-1);
   y3(i) = y3(i-1) + k1b;
   yb(i) = ((3*L)- y3(i))*10^(3);
   F2(i) = ((a2*(yb(i)^4)) + (b2*(yb(i)^3)) + (c2*(yb(i)^2)) + (d2*yb(i)) + e2)-(c*y4(i-1));
   k2b = h*((F2(i)/(m1+m2)) - g);
   y4(i) = y4(i-1) + k2b;
else
   y3(i) = 3*L;
   y4(i) = 0;
end

if(y5(i-1)<(5*L))
   k1c = h*y6(i-1);
   y5(i) = y5(i-1) + k1c;
   yc(i) = ((5*L)- y5(i))*10^(3);          %in mm
   F3(i) = ((a3*(yc(i)^4)) + (b3*(yc(i)^3)) + (c3*(yc(i)^2)) + (d3*yc(i)) + e3)-(c*y6(i-1));
   Fs(i) = 2*k*yc(i)*10^(-3);
   Fsum(i) = F3(i) + Fs(i);
   k2c = h*((Fsum(i)/(m1+m2+m3)) - g);
   y6(i) = y6(i-1) + k2c;
else
   y5(i) = 5*L;
   y6(i) = 0;
end
          ysum(i) = (y1(i)) + (y3(i)-L) + (y5(i)-(3*L));
end
%plot(t,ysum)
data = [t; ysum*100];
fid = fopen('Allsolenoids.txt','wt');
fprintf(fid,'%12.8f\t%12.8f\n',data);
fclose(fid)
%hold on
%plot(t,y3)
%hold on
%plot(t,y5)
```